ISSN 1560-3547, Regular and Chaotic Dynamics, 2012, Vol. 17, No. 5, pp. 451–478. © Pleiades Publishing, Ltd., 2012.

Bifurcation Analysis and the Conley Index in Mechanics[1]

Alexey V. Bolsinov[1,2*], Alexey V. Borisov[2], and Ivan S. Mamaev[2***]**

[1]*School of Mathematics, Loughborough University*
United Kingdom, LE11 3TU, Loughborough, Leicestershire

[2]*Institute of Computer Science, Udmurt State University,*
ul. Universitetskaya 1, Izhevsk, 426034 Russia

Received 21 September, 2011; accepted 10 April, 2012

Abstract—The paper is devoted to the bifurcation analysis and the Conley index in Hamiltonian dynamical systems. We discuss the phenomenon of appearance (disappearance) of equilibrium points under the change of the Morse index of a critical point of a Hamiltonian. As an application of these techniques we find new relative equilibria in the problem of the motion of three point vortices of equal intensity in a circular domain.

MSC2010 numbers: 76M23, 34A05

DOI: 10.1134/S1560354712050073

Keywords: Morse index, Conley index, bifurcation analysis, bifurcation diagram, Hamiltonian dynamics, fixed point, relative equilibrium

Contents

[1]Originally published in Russian in *Russian Journal of Nonlinear Dynamics*, 2011, vol. 7(3), pp. 649–681.

[*]E-mail: A.Bolsinov@lboro.ac.uk

[**]E-mail: borisov@rcd.ru

[***]E-mail: mamaev@rcd.ru

1. INTRODUCTION

In this paper we follow the same idea as in our recent papers [2, 3], namely, to demonstrate how the constructions well known in pure mathematics (in particular, in topology) can be used in problems of mechanics. It happens quite often that such constructions are not used by specialists in applications because of too abstract language. We would like to explain these in a less formal language, bearing in mind not only methodical and educational purposes but mainly expanding and developing the interaction between various branches of mathematics and mechanics. As in our previous papers, we first expose some theoretical material, and then illustrate it with an example from mechanics. As a new application we give the description of relative equilibria in one of the problems in vortex dynamics. In mechanics, it is often required to analyze the properties of singular points of a Hamiltonian depending on some parameters. It is well-known that a nondegenerate (in the sense of Morse theory) singular point is stable with respect to small perturbations of a parameter: it remains nondegenerate and its index does not change. However, for some (bifurcational) values of the parameter degenerations can occur, and while passing through them the index of a singular point may change. In such cases it is important to understand the scenarios of possible bifurcations. One of the questions which turn out to be important in this context (e.g., if one needs to analyze relative equilibria) is as follows: can the index of an isolated equilibrium point change without giving rise to new equilibria? The most suitable mathematical tool to answer this kind of questions is the Conley index, which is the topological invariant of an isolated invariant set of a dynamical system. It was introduced and studied by Charles Conley in the 1960s–1970s of the past century [21]. The efficiency of this invariant in various problems of dynamical systems theory is very well known to experts [20] involved in this field, but it cannot be said that this concept is familiar to specialists in applied areas. The following section is devoted to the definition of the Conley index and simplest constructions related to it (see also [29, 30, 1]).

2. THE CONLEY INDEX: MOTIVATION, DEFINITION AND EXAMPLES

Before giving a formal definition of the Conley index, we remind the reader of some elementary concepts from topological dynamics (see, e.g., [5, 18, 28]).

2.1. The Index of a Vector Field and the Morse Index

a. The index of a vector field. Let a dynamical system $\dot{\boldsymbol{x}} = \boldsymbol{v}(\boldsymbol{x})$ be given on the plane $\mathbb{R}^2$ in some region U whose boundary is a smooth closed curve $\gamma(t)$, $t \in [0, 2\pi]$, $\gamma(0) = \gamma(2\pi)$. Suppose there are no equilibrium points at the boundary of U, i.e. $\boldsymbol{v}(\boldsymbol{x}) \neq 0$ for all $\boldsymbol{x} \in \gamma$. Can we find out from the behavior of the vector field at the boundary of the region whether there exists an equilibrium point inside the region? The *index of the vector field* serves as a good tool to answer this question. The index is defined as follows.

Consider the vector field $\boldsymbol{v}$ at the boundary as a periodic vector function $\boldsymbol{v}(t) = \boldsymbol{v}(\gamma(t))$ of the parameter t on the curve γ. The *index of the vector field* $\boldsymbol{v}$ (ind $\boldsymbol{v}$) at the boundary γ of the region U is the number of revolutions made by the vector $\boldsymbol{v}(t)$ when passing round along the boundary, i.e. under the change of t from 0 to 2π (Figs. 1 and 2).

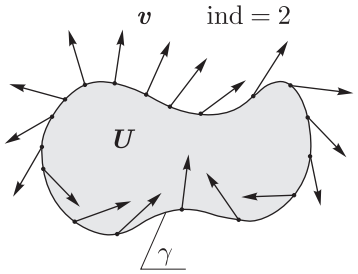

Fig. 1

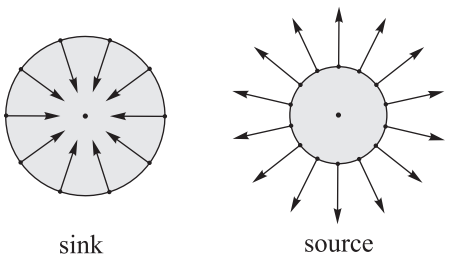

Fig. 2

Theorem 1. *If the index is different from zero, an equilibrium point (fixed point) of the dynamical system exists necessarily inside the region U. Conversely, if the index is equal to zero, the vector field $\boldsymbol{v}$ can be extended from the boundary into the region U in such a way that there will be no equilibrium points inside.*

Remark 1. If the curve $\gamma(t)$ and the vector field $\boldsymbol{v}(t)$ on it have a certain degree of smoothness, then the field $\boldsymbol{v}$ can also be extended into the region with the same degree of smoothness. In the analytical case, a real-analytic extension is also possible.

It is straightforward to generalize this definition to the multidimensional case. If we have a region $U \subset \mathbb{R}^n$ homeomorphic to the ball B^n, with boundary ∂U diffeomorphic to the unit sphere $S^{n-1} \subset \mathbb{R}^n$, and the vector field $\boldsymbol{v}$ at the boundary does not vanish, then one can determine the natural mapping $\phi\colon \partial U \to S^{n-1}$, setting $\phi(\boldsymbol{x}) = \boldsymbol{v}(\boldsymbol{x})/|\boldsymbol{v}(\boldsymbol{x})|$. The *index of the vector field* is the degree of this mapping. In particular, if ϕ is a one-to-one mapping, the index is equal to ± 1.

Remark 2. We recall the formal definition of the degree of mapping. Suppose there is a smooth mapping $F\colon \mathcal{M}_1 \to \mathcal{M}_2$ between two compact oriented manifolds of equal dimension. Then for almost any point $\boldsymbol{y} \in \mathcal{M}_2$ its inverse image F^{-1} contains only a finite number of points $\boldsymbol{x}_1, \ldots, \boldsymbol{x}_m$, all of them being regular, i.e. the determinant of the Jacobi matrix of F at each of these points is different from zero. By definition, the degree of mapping F is the number

$$\deg F = \sum_{\boldsymbol{x}_i \in F^{-1}(\boldsymbol{y})} \operatorname{sign} \det dF(\boldsymbol{x}_i).$$

In other words, the degree of mapping is the number of inverse images of a regular point counted taking into account the sign of each point, which is defined by whether the mapping F preserves or changes orientation. The degree of mapping possesses two fundamental properties: it does not depend on the choice of the regular point $\boldsymbol{y}$, which is used in the definition, and, in addition, the degree of mapping does not change under a continuous deformation of the mapping F.

As one of the most typical examples we can consider the complex polynomial $f(z)$ of degree n regarded as a mapping of the extended complex plane $\overline{\mathbb{C}}$ into itself. From the topological point of view $\overline{\mathbb{C}}$ is a two-dimensional sphere S^2 (the so-called Riemann sphere), and the degree of mapping $f\colon \overline{\mathbb{C}} \to \overline{\mathbb{C}}$ is equal to the degree of polynomial, since for the point w_0 of general position the equation $f(z) = w_0$ has n various solutions $z_1, \ldots, z_n$, with the signs at all points being positive, since for any complex mapping $f(z) = u(x, y) + iv(x, y)$ at a regular point we have $\det df = \left\| u_x \;\; u_y \;\; v_x \;\; v_y \right\| = u_x^2 + u_y^2 = |f'(z)|^2 > 0.$

The index of the vector field possesses two remarkable properties.

1) it does not change under a deformation of the region U if in the process of deformation the boundary of the region does not pass through equilibrium points.

2) the index does not change in the process of deformation of the dynamical system itself. In other words, if the vector field $\boldsymbol{v}(\boldsymbol{x}) = \boldsymbol{v}_0(\boldsymbol{x})$ is included in the family $\boldsymbol{v}_\alpha(\boldsymbol{x})$ continuously depending on the parameter α, then the index $\boldsymbol{v}_\alpha$ at the boundary ∂U does not depend on α (of course, on the condition that no equilibrium points arise in the process of deformation at the boundary of the region).

Theorem 1 for the multidimensional case is valid in the same formulation.

The index of an isolated singular point $\boldsymbol{x}_0$ of a vector field $\boldsymbol{v}(\boldsymbol{x})$ is the index for the boundary of its small spherical neighborhood (this neighborhood must, of course, not contain any other singular points). The following simple property of summation is valid:

> *if there are several isolated singular points inside a region, then the index along the boundary of the entire region is equal to the sum of indices of individual points.*

Remark 3. The index of a vector field is also often called the Poincaré – Hopf index, since it is well known primarily due to the Poincaré – Hopf theorem stating that the sum of indices of singular points of a vector field on a compact manifold is equal to its Eulerian characteristic. Poincaré proved this theorem for two-dimensional manifolds, and Hopf generalized it to the multidimensional case.

A disadvantage of this index is its small informativeness. For example, if we consider the gradient vector field of the simplest quadratic function $f = \pm\frac{1}{2}(x^2 + y^2)$

$$\boldsymbol{v} = \operatorname{grad} f = \pm(x, y), \tag{2.1}$$

then its index is equal to 1 regardless of the choice of sign and therefore does not allow one to distinguish between the sink and the source (Fig. 2). And in general, in the case of a nondegenerate singular point of a vector field in $\mathbb{R}^n$ its index is always equal to ± 1, although such points can have significantly different topological types. Thus, for example, in Fig. 1 ind $= 2$, this means that inside the region there is something more complex than a nondegenerate singular point. However, it is impossible to determine what exactly is located there. There can, for example, be an isolated singular point there, but then it has to be degenerate. Or there can be several nondegenerate singular points there (e.g., two sinks or two sources). Examples are given in Fig. 3.

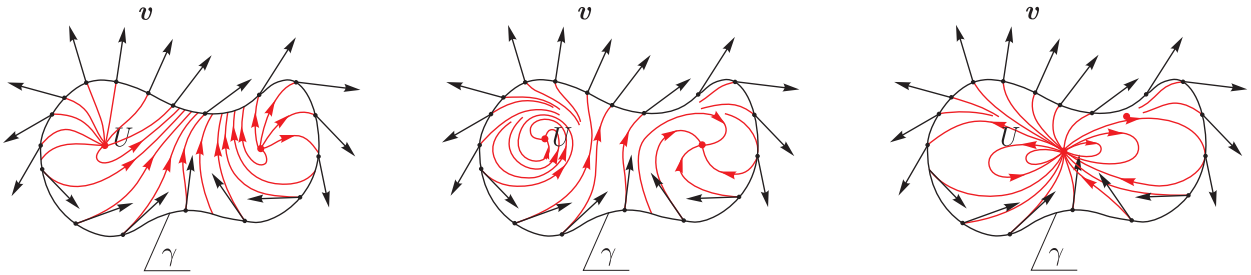

Fig. 3

b. The Morse index. For the above example of the gradient flow (2.1) the *Morse index* of the singular point of the corresponding smooth function is more informative. We remind the reader of this construction. Let $f(\boldsymbol{x})$, $\boldsymbol{x} \in \mathbb{R}^n$, be a smooth function and $\boldsymbol{x}^{(0)}$ be its nondegenerate singular point (recall that this means: $\det \left(\dfrac{\partial^2 f}{\partial x_i \partial x_j}\right)\Big|_{\boldsymbol{x}^{(0)}} \neq 0$).

The negative index of inertia of the second differential $\left(\dfrac{\partial^2 f}{\partial x_i \partial x_j}\right)$ is called the index of the singular point $\boldsymbol{x}^{(0)}$. In other words, if the second differential is brought to a normal form via a linear change so that

$$f(\boldsymbol{x}) = f(\boldsymbol{x}^{(0)}) - x_1^2 - \ldots - x_k^2 + x_{k+1}^2 + \ldots + x_n^2 + \ldots,$$

then the Morse index is the number k.

The relation of the usual index ind of a singular point of the field $\boldsymbol{v} = \operatorname{grad} f$ with the Morse index ind_M is very simple:

$$\operatorname{ind} \operatorname{grad} f(\boldsymbol{x}^{(0)}) = (-1)^{\operatorname{ind}_M f(\boldsymbol{x}^{(0)})}. \tag{2.2}$$

In the case of the Hamiltonian vector field on $\mathbb{R}^{2n} = \{(\boldsymbol{q}, \boldsymbol{p})\}$ determined by the equations

$$\dot{\boldsymbol{q}} = \frac{\partial H}{\partial \boldsymbol{p}}, \quad \dot{\boldsymbol{p}} = -\frac{\partial H}{\partial \boldsymbol{q}}, \tag{2.3}$$

for a nondegenerate fixed point $\boldsymbol{x}^{(0)} = (\boldsymbol{q}, \boldsymbol{p})$ there is an analogous invariant — the Morse index of the Hamiltonian $H(\boldsymbol{q}, \boldsymbol{p})$ at the point $\boldsymbol{x}^{(0)}$. It is interesting to note that the indices of the

Hamiltonian vector field (2.3) and the gradient field grad H coincide (and are determined by (2.2)), since the vector fields are related to each other by a nondegenerate operator with a positive determinant.

For vector fields of arbitrary nature in the case of hyperbolic singular points the Morse index [1] can also be defined. From the viewpoint of dynamics *the Morse index of a hyperbolic singular point* (or a closed trajectory) of a dynamical system is defined as the dimension of the unstable invariant manifold. In particular, the Morse index of the vector field grad f at a nondegenerate singular point is equal to the Morse index of the function $-f$ at this point.

The Morse index gives a better understanding of the behavior of the system near an equilibrium point. However, its shortcoming is that it is well defined only for nondegenerate singular points. Its stability under the deformation of the function $f_0(\boldsymbol{x}) \rightsquigarrow f_\alpha(\boldsymbol{x})$ is difficult to judge for the simple reason that for some values of the parameter α the nondegeneracy condition is violated and at this moment the index cannot be determined at all. In addition, the vector field can exhibit more complex invariant subsets (submanifolds) than a fixed point, which one would also like to characterize by means of some invariant.

Therefore, one would like to have a generalization of the Morse index which could be used in the case of degenerations as well. The Conley index is just such an invariant. Unlike the two previous indices, the Conley index is not a number but a topological space. And even not a space but its homotopy type. In order to define it, we will need some topological definitions.

2.2. Preliminary Considerations

Although intuitively the idea of the Conley index is simple and natural, a formal definition may at first glance seem strange and even artificial. In this section we discuss preliminary constructions motivating the choice of this invariant.

Let us consider a neighborhood N of an isolated singular point of a dynamical system ϕ^t and mark out at its boundary an *exit set* L consisting of those points where the trajectories leave the neighborhood. In a sense, this pair (N, L) characterizes the dynamics near a singular point (roughly speaking, it shows which part of the flow goes out from the neighborhood). When both the system ϕ^t and the neighborhood N are slightly perturbed, the topology should not change, therefore, one would like to regard the pair (N, L) as a topological invariant of the singularity.

However, such a naive definition does not satisfy the natural requirements for invariants. Thus, for example, it depends significantly on the form of the neighborhood (an example is shown in Fig. 4). We note that a priori no additional restrictions can be imposed onto the neighborhood, since it is difficult to keep track of its form (with respect to the flow) in the process of deformation.

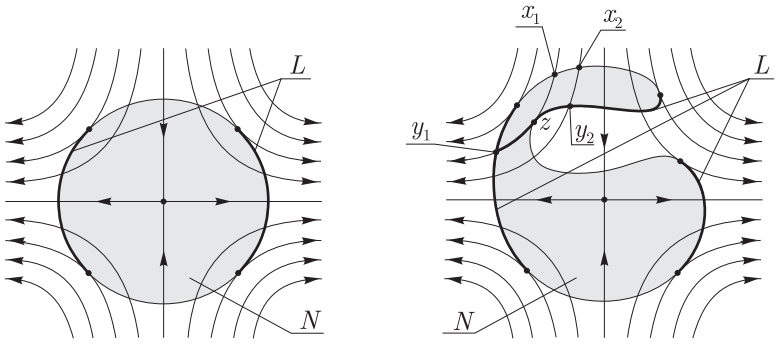

Fig. 4. Examples of various neighborhoods of the fixed point of a flow.

Another idea which is used in the construction of the Conley index to avoid this disadvantage is to shrink the neighborhood N along the flow toward the exit set L. Formally, this implies a mapping — a half-flow which is defined as follows: each point $\boldsymbol{x} \in N$ moves along its trajectory in the positive direction until it reaches the exit set L, then it stops immediately. In particular, the

points belonging to L remain fixed and do not move anywhere, and the points that never reach the exit keep moving along their usual trajectories up to infinity, i.e. if there is an invariant set inside the neighborhood, it remains unchanged, and the entire remaining part N sticks to the exit set L.

But this half-flow has also a shortcoming: it is not continuous. This is clearly seen in the example in Fig. 4b: the points $\boldsymbol{x}_1$ and $\boldsymbol{x}_2$ are close but leave the neighborhood at the points $\boldsymbol{y}_1$ and $\boldsymbol{y}_2$, which are far apart. To avoid this trouble, we have to include the point $\boldsymbol{z}$ in the set L. But this will not be sufficient either. There will be a problem with those points which lie on the trajectory between $\boldsymbol{z}$ and $\boldsymbol{y}_1$. The point $\boldsymbol{z}$ itself is already an exit point and, therefore, should not move anywhere, while the other points on the segment of the trajectory must be deformed into the point $\boldsymbol{y}_1$. The solution of the problem is to include in the set L all points located on the trajectory between $\boldsymbol{z}$ and $\boldsymbol{y}_1$. In other words, the following requirement is important: if some point has reached the exit set L, then this point must not leave it and go to $N \setminus L$ again [1)]. Moreover, since the dynamics on the exit set is ignored, it turns out to be necessary to contract the entire exit set L to one point for the sake of continuity; we shall denote such a space arising from the pair (N, L) by N/L (see the following section for more details).

There is another important point. As is well known from examples, there may arise new equilibrium points and closed trajectories or more complex invariant sets in the process of deformation. For this reason it makes sense not to confine our attention to the equilibrium points but to consider from the very beginning *invariant* (i.e. consisting of whole trajectories) *compact subsets* S of arbitrary nature. The requirement for the invariant set S is that it must be *isolated*, i.e. there must exist such a neighbourhood N (it is more convenient to regard this neighbourhood as compact) in which S is the maximal invariant subset. Such a neighbourhood is called *isolating*.

It is interesting to note that the definition of an isolating neighborhood N can be given using the properties of the flow ϕt only in a neighborhood of the boundary ∂N without mentioning the set S itself (which may actually turn out to be empty, and this case should not by any means be excluded from consideration):

> a compact set N is called an *isolating neighbourhood* if no boundary point $\boldsymbol{x} \in \partial N$ lies on a trajectory entirely contained in N.

Remark 4. A point of center type on the plane (in whose neighborhood all trajectories are closed) has no isolating neighborhood. Under small deformation the center can turn both into a sink and into a source.

The above considerations justify the conditions on L formulated below. Before giving a formal definition for the Conley index, we recall some basic facts from elementary topology.

2.3. Necessary Facts from Elementary Topology

Assume that X is a topological space and $Y \subset X$ is its compact subset. Let X/Y denote a new topological space obtained from X by contracting Y to a point. Examples are shown in Fig. 5.

Fig. 5a: if we "contract" to a point (i.e. identify) the ends $\{0\} \cup \{1\} = Y$ of the segment $X = [0, 1]$, then we obtain a circle as X/Y;

Fig. 5b: if we contract the half Y of the disk X to a point, then we again obtain a disk;

Fig. 5c: if we contract the parallel Y on the torus X to a point, then the space X/Y will be the pinched torus;

Fig. 5d: if we contract the boundary circle Y of the two-dimensional disk X to a point, then we obtain a two-dimensional sphere.

[1)] Recall that $N \setminus L$ denotes the complement to L in N, i.e. $N \setminus L = \{\boldsymbol{x} \in N, \boldsymbol{x} \notin L\}$.

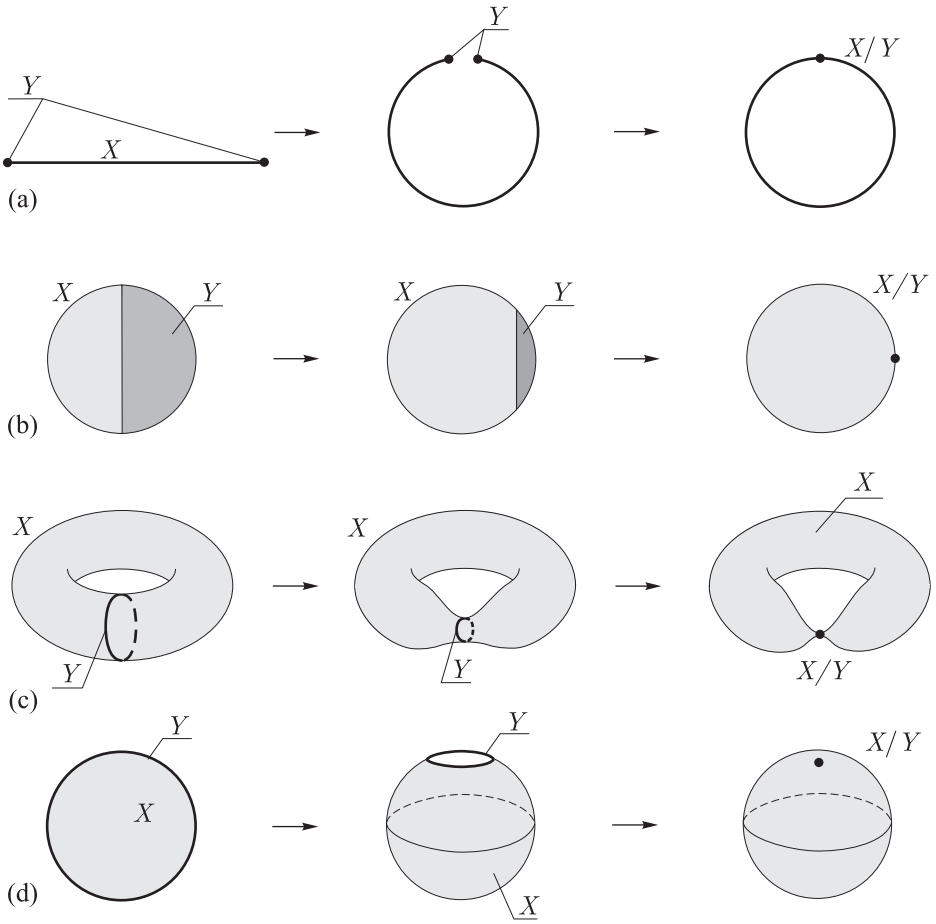

Fig. 5. Examples of spaces X/Y.

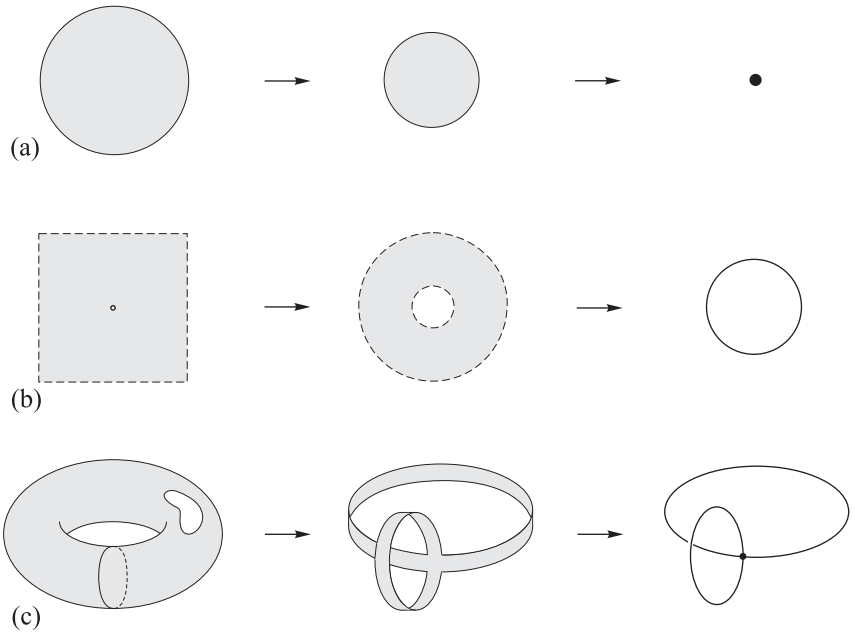

Fig. 6. Examples of homotopically equivalent spaces.

The last example has a natural multidimensional generalization: if X is an n-dimensional ball and Y is its boundary sphere, then by contracting it to a point we obtain the space X/Y homeomorphic to an n-dimensional sphere.

Furthermore, after contracting the subset Y to a point we obtain in the space X/Y some marked point, which we shall denote by $[Y]$.

Two topological spaces X_1 and X_2 are called *homotopically equivalent* if they can be "deformed" into each other. Examples are shown in Fig. 6:

Fig. 6a: an n-dimensional ball is homotopically equivalent to a point;

Fig. 6b: a punctured plane is homotopically equivalent to a circle;

Fig. 6c: a torus with a hole is homotopically equivalent to the bouquet of two circles (i.e. two circles glued together at one point).

For a more rigorous definition of the concept of homotopic equivalence one should first introduce the concept of *homotopic mappings*. Let $f_0, f_1 \colon X \to Y$ be two continuous mappings. They are called homotopic if there exists a continuous family of mappings $f_\alpha \colon X \to Y$, $\alpha \in [0,1]$ deforming one mapping into another. More formally, there exists a continuous mapping $F \colon X \times [0,1] \to Y$ such that $f_0(\boldsymbol{x}) = F(\boldsymbol{x}, 0)$, $f_1(\boldsymbol{x}) = F(\boldsymbol{x}, 1)$ for $\boldsymbol{x} \in X$.

Topological spaces X_1 and X_2 are called *homotopically equivalent* (or having the same *homotopy type*) if there exist two maps $f \colon X_1 \to X_2$ and $g \colon X_2 \to X_1$ such that $f \circ g \colon X_2 \to X_2$ is homotopic to the identity map id_{X_2} and $g \circ f \colon X_1 \to X_1$ is homotopic to the identity map id_{X_1}.

A less trivial example: Let X be a 3-dimensional ball and Y be a circle on the boundary sphere. What is the homotopy type of the space X/Y? The deformation in Fig. 7 shows that X/Y has the homotopy type of the two-dimensional sphere S^2.

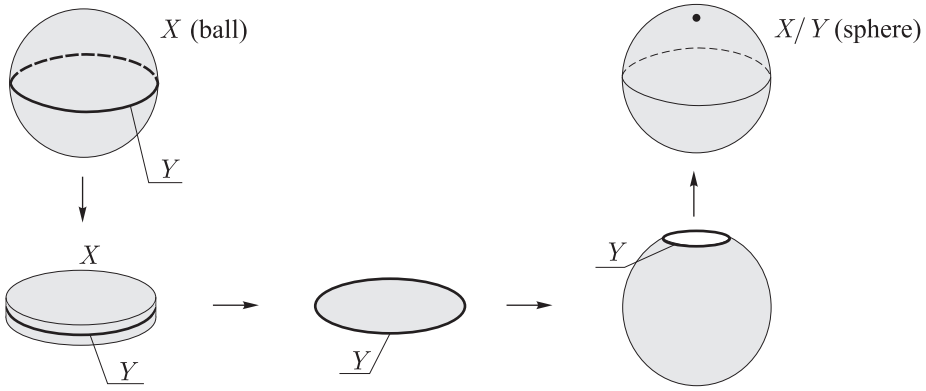

Fig. 7. The process of deformation of a ball with a marked circle into a sphere.

2.4. Formal Definition

Let a dynamical system $\phi^t \colon X \to X$ be given on some manifold X (as X one can consider an arbitrary locally compact topological space). A compact invariant subset $S \subset X$ is called *isolated* if for this subset there exists a compact neighbourhood N in which S is the maximal invariant subset (in other words, S is the invariant part of N):

$$S = \mathrm{inv}\,(N) := \{\boldsymbol{x} \in N \colon \phi^t(\boldsymbol{x}) \in N \ \text{ for all } \ t \in \mathbb{R}\}.$$

In this case, N is called an *isolating neighbourhood* for S. The Conley index assigns to S the homotopy type of some topological space with a marked point. The construction is as follows.

The *index pair* (N, L) for the isolated invariant set S consists of two compact subsets $L \subset N$ of the manifold X such that

— the closure of the set $N \setminus L$ is an isolating neighbourhood for S;

— L is an exit set for N: for any $\boldsymbol{x} \in N$ and $t > 0$ with the condition $\phi^t(\boldsymbol{x}) \notin N$ there exists $t_0 \in [0, t]$ such that $\phi^{t_0}(\boldsymbol{x}) \in L$;

— L is positively invariant in N, i.e. the points which have reached L, cannot "escape back" into $N \setminus L$: if $\boldsymbol{x} \in L$ and $\phi^\tau(\boldsymbol{x}) \in N$ for all $\tau \in [0, t]$, $t > 0$, then $\phi^t(\boldsymbol{x}) \in L$.

It can be shown that an index pair exists for every invariant isolated set S. Moreover, if (N, L) and (N', L') are two index pairs for S, then the factor spaces N/L and N'/L' are homotopically equivalent as spaces with the marked points $[L]$ and $[L']$.

Definition 1. *The Conley index* $\mathrm{ind}_C(S, \phi)$ *of the invariant set S of the flow ϕ^t is the homotopy type of the space N/L with the marked point $[L]$, where (N, L) is an index pair for S.*

Furthermore, as was stated in the previous section, the isolating neighbourhood and, consequently, the index pair (N, L) can be correctly defined for the flow ϕ^t without using an invariant set. For this reason, the topological type of N/L will also be called *the Conley index of the isolating neighborhood* $\mathrm{ind}_C(N, \phi)$. The invariant set itself need not be mentioned at all. Conceptually this is very important, since in many cases we do not know anything about this invariant set lying inside the neighborhood.

The index defined in this way possesses three fundamental properties.

Theorem 2 (The Conley theorem). *Let N be an isolating neighbourhood of some smooth dynamical system. Then*

1) *the index is an invariant of isolating neighborhoods;*

2) *if the index is nontrivial, i.e. different from a "point", then inside the isolating neighborhood there is a nonempty invariant set;*

3) *if ϕ_α is a continuous family of dynamical systems for each of which N is an isolating neighbourhood, then the index* $\mathrm{ind}_C(N, \phi_\alpha)$ *is the same for all values of the parameter α.*

Remark. In this (or the most close) formulation the above theorem is presented in [30].

Thus, according to these properties, if there are two different isolating neighbourhoods of the same invariant set, then the index does not depend on which of these neighborhoods we shall consider. Moreover, this invariant set S itself is not important at all: any events can happen to it inside this neighborhood under a deformation (for example, it can completely disappear), but the index will not change.

For our purposes, the most important is the third property of the Conley index, namely, its stability under deformation of a dynamical system. It is often applied in the following situation. Assume that we are given two dynamical systems ϕ_0 and ϕ_1 included in a continuous family ϕ_α. Let N be an isolating neighbourhood for ϕ_0 and ϕ_1. Then two cases are possible:

- either the Conley index remains the same under a change of the parameter α, and, in particular, $\mathrm{ind}_C(N, \phi_0) = \mathrm{ind}_C(N, \phi_1)$;

- or the index has changed and then, for some intermediate value of the parameter $\alpha \in (0, 1)$ the neighbourhood N has ceased to be isolating.

Recall that the violation of the condition of being isolating is equivalent to the existence of a boundary point $\boldsymbol{x} \in \partial N$ such that the trajectory passing through it is entirely contained in N.

Remark. If the condition of being isolating is violated for some value of α, Conley's theory ceases to work and cannot give a definite answer as to whether or not the index will change.

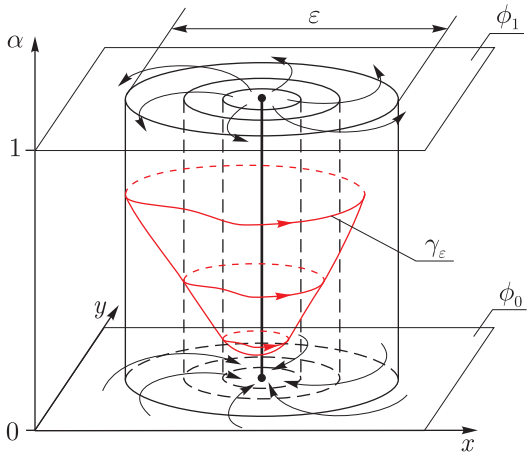

Fig. 8. The Andronov – Hopf bifurcation.

c. The Andronov – Hopf bifurcation [24]. One of the most illustrative examples of application of these properties is the *bifurcation of the birth of a cycle* on a plane when for each value of the parameter $\alpha \in [0, 1]$ there is exactly one stationary point with complex multipliers $\lambda(\alpha) \pm i\mu(\alpha)$. The bifurcation implies that the real part of the multiplier, i.e. $\lambda(\alpha)$, changes sign from minus to plus, resulting in the attracting point turning into a repulsive one. The Conley index changes from a pair of points at $\lambda < 0$ to a pointed sphere at $\lambda > 0$ (see the example below in Figs. 9a and 9c). Hence, if the standard ε-neighbourhood of the point is fixed in such a way that it is isolating for both $\alpha = 0$ and $\alpha = 1$, then for some intermediate value of the parameter α it will cease to be isolating, and this will mean that a closed trajectory entirely lying in this neighborhood passes through some boundary point of the neighborhood. It is clear that this is a limit cycle, since there can be nothing else for dimensional reasons. Such a trajectory (at various values of the parameter α) exists for any ε. We denote it by γ_ε. It is obvious that all these trajectories are different and form a family of closed cycles (see Fig. 8). Thus, we obtain a proof of the existence of a family of closed trajectories.

2.5. Examples of the Conley Index

In most examples, as an isolating neighborhood N one can take the most natural (compact) neighborhood of an invariant set, and as a subset $L \subset N$ one can consider the usual exit set lying at the boundary ∂N.

a. A source, a saddle and a sink on a plane. Figure 9 shows the corresponding index pairs. In all cases, a disk with its center at an equilibrium point is taken as N, and the exit set L consists:

(a) in the case of a source — of a whole boundary circle,

(b) in the case of a saddle — of two arcs,

(c) in the case of a sink — it is empty.

If the boundary circle of the disk is contracted to a point, we obtain a two-dimensional sphere (Fig. 9a). If two arcs are identified into a point, we obtain a space which is homotopically equivalent to a circle (Fig. 9b). In the case of a source the exit set is empty; formally "shrinking it to a point", we obtain a point lying separately from the disk N (this rule is adopted as a convention). Thus, the factor space N/L is the disjoint union of the disk and the point. Since the disk is homotopically equivalent to a point, the Conley index in the case of a sink is the homotopy type of a space consisting of a pair of points (or, what is the same, a zero-dimensional sphere $S^0 = \{\boldsymbol{x}^2 = 1, \boldsymbol{x} \in \mathbb{R}\}$).

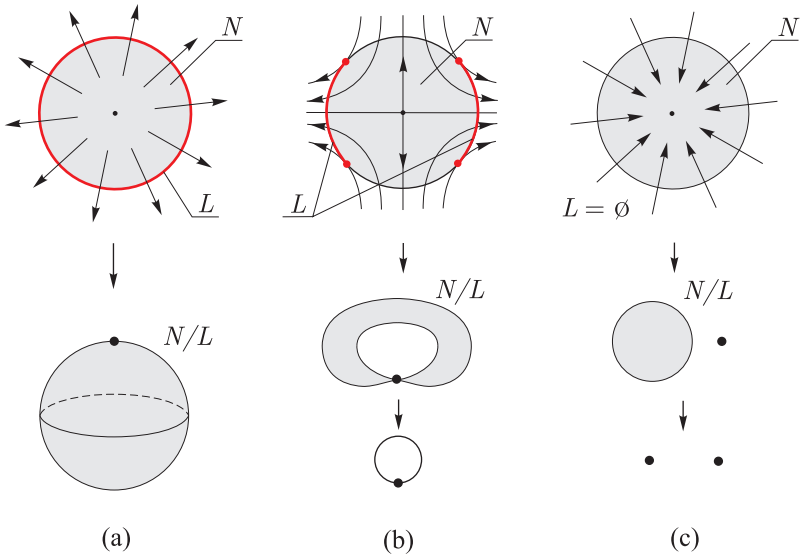

Fig. 9. The Conley index for a source, a saddle and a sink.

It is useful to observe what will happen if the form of the isolating neighborhood changes. For example, as shown in Fig. 10. The exit set at the boundary of this neighborhood consists of three components. However, one of them is not closed. If one considers its closure, i.e. adds one point, the property of positive invariance is violated. This problem can easily be avoided by adding a piece of the trajectory marked in Fig. 10. After these modifications N and L satisfy the definition of an index pair. If L is contracted to a point, we obtain a space shown in Fig. 10. It is easily seen that despite a rather big difference between this index pair and the standard one, the Conley index does not change: as before, the resulting factor space N/L is homotopically equivalent to a circle.

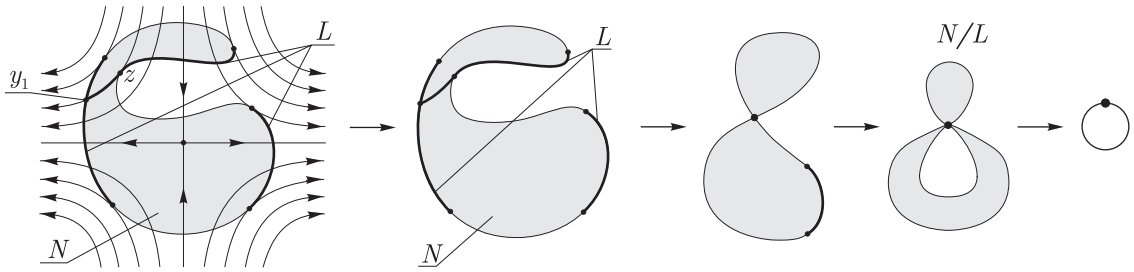

Fig. 10

b. Two saddles and a separatrix connecting them. The index pair (N, L) of this invariant set is shown in Fig. 11, the Conley index is the homotopy type of the union of two circles.

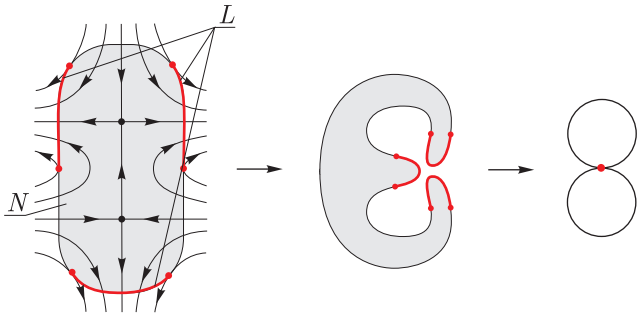

Fig. 11. The Conley index of a pair of saddles connected by a separatrix.

It is interesting to note the following. One can deform this system in such a way that the separatrix between the two saddles splits into two separatrices passing by each other, in this case the invariant set will change: now it consists of two points (Fig. 12a). Notice that the Conley index will remain the same. This is quite natural, since the index pair has not changed at all. Much more interesting is the fact that as a different index pair we can now take two individual neighborhoods of these points (Fig. 12b). In this case, four arcs will be the exit set L; nevertheless, the Conley index will not change in any way.

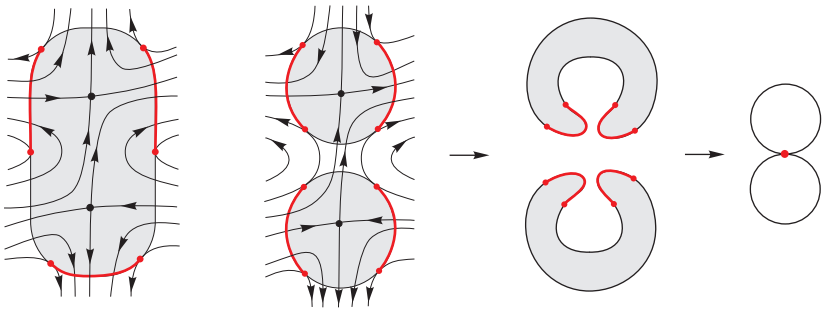

(a) (b)

Fig. 12. The Conley index of a pair of unconnected saddles.

c. The gradient flow of a Morse function. Consider an important example which allows one to relate the Morse index and the Conley index to each other — the gradient flow of a Morse function with a nondegenerate singular point of the index k:

$$f(\boldsymbol{x}) = -x_1^2 - \cdots - x_k^2 + x_{k+1}^2 + \cdots + x_n^2,$$
$$\dot{\boldsymbol{x}} = \mathbf{B}\boldsymbol{x}, \quad \mathbf{B} = \operatorname{diag}(\underbrace{-1,\ldots,-1}_{k},\underbrace{1,\ldots,1}_{n-k}).$$

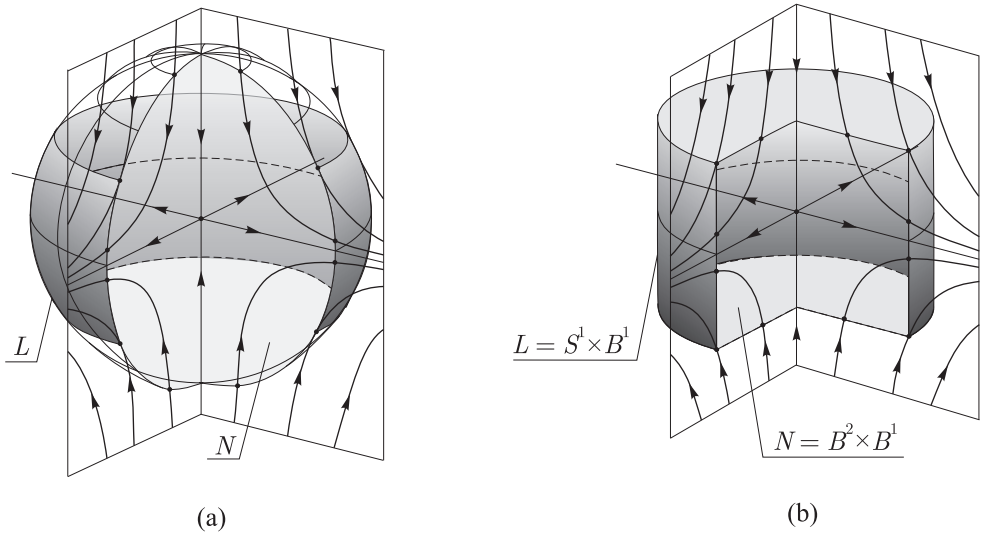

(a) (b)

Fig. 13. Cross-sections of an axisymmetric flow in a neighborhood of a saddle singular point and possible isolating neighborhoods. (The darker color on the boundary of the isolating neighbourhoods shows the exit set.)

If $k \neq 0$, then this singular point is hyperbolic, its stable and unstable manifolds have dimensions $n-k$ and k. The set N in the index pair is a spherical neighbourhood of the singular point and the exit set L lying on the boundary of the $n$frm[o]–dimensional ball N is the direct product of a sphere of dimension $k-1$ and a disk of dimension $n-k$. An example for $n=3$, $k=2$ is shown in Fig. 13a.

The index pair shown in the figure can be changed by taking a three-dimensional cylinder as N and its lateral surface (Fig. 13b) as L. In the general case one can take the direct product of two disks $N = B^k \times B^{n-k}$ as N and the lateral surface $S^{k-1} \times B^{n-k} = \partial B^k \times B^{n-k}$ as L. Homotopically the second factor B^{n-k} in these direct products is trivial and plays no role, therefore, by contracting L (i.e. actually the boundary sphere S^{k-1} of the ball B^k) to a point, we obtain a k-dimensional sphere.

Thus, the Conley index of a singular point of the gradient flow of a Morse function of index k is the homotopy type of the k-dimensional sphere.

3. APPLICATION TO THE PROBLEM OF RELATIVE EQUILIBRIA

3.1. The Change of the Index and the Birth of Equilibrium Points

Consider a system whose Hamiltonian $H(\boldsymbol{x}, \alpha)$ is a smooth function on $\mathbb{R}^n$ depending on a parameter $\alpha \in [-1, 1]$. Let $\boldsymbol{x}_0 \in \mathbb{R}^n$ be its nondegenerate singular point at $\alpha = -1$. What happens to this point under a change of the parameter? It is well known that under a small variation of the parameter it remains nondegenerate and its Morse index does not change (the point itself can, of course, slightly change its location). Moreover, as long as it remains nondegenerate, its index remains the same. This easily follows from the continuity argument and the implicit function theorem. The following natural question arises:

can the Morse index of the point change during a passage through degeneration, and if it can, what does this change imply?

Consider two examples.

The first example is quite simple:

$$H(q, p; \alpha) = \alpha(p^2 + q^2).$$

As α passes through zero, the index of the singular point $(0, 0)$ changes: $\mathrm{ind}_M{=}2 \mapsto \mathrm{ind}_M{=}0$. However, at $\alpha = 0$ the function H becomes identically zero, and the singular point $(0, 0)$ is not isolated. It is clear that such a situation is not generic, and for this reason, as a rule, does not occur in applications.

The second example is:

$$H(q, p; \alpha) = p^2 - \alpha q^2 + q^4. \tag{3.1}$$

Here after the passage of α through zero the index of the singular point $(0, 0)$ changes from 1 to zero and the point $(0, 0)$ is isolated for each value of the parameter. In other words, we have a smooth one-parameter (the parameter is α) family of points $\boldsymbol{x}^{(0)}(\alpha) = (0, 0)$ in which the index changes passing through degeneration at $\alpha = 0$. We note that the change of the index implies here the appearance of new singular points: at $\alpha > 0$ there are two more families of singular points $\boldsymbol{x}^{(1)}(\alpha) = \left(0, \sqrt{\dfrac{\alpha}{2}}\right)$, $\boldsymbol{x}^{(2)}(\alpha) = \left(0, -\sqrt{\dfrac{\alpha}{2}}\right)$.

Such a situation is inevitable: if the index has changed, then in an arbitrarily small neighborhood of the family of singular points there must exist other singular points. Namely, the following theorem holds.

Theorem 3. *Let $H(\boldsymbol{x}, \alpha)$ be a smooth function on $\mathbb{R}^n$ smoothly depending on a parameter $\alpha \in [-1, 1]$ and let $\boldsymbol{x}_0 \in \mathbb{R}^n$ be an isolated singular point of $H(\boldsymbol{x}; \alpha)$ for each α. Let $\boldsymbol{x}_0$ be nondegenerate at $\alpha \neq 0$ and let its Morse index change as α passes through zero. Then in an arbitrarily small neighborhood of $\boldsymbol{x}_0$ there exist other singular points for some values of α.*

Remark. In this theorem one can, of course, assume that the singular point $\boldsymbol{x}_0$ is not fixed but smoothly depends on α.

The Proof follows in an obvious way from the properties of the Conley index. Since the point $\boldsymbol{x}_0$ is nondegenerate for $\alpha = \pm 1$, it is isolated, and for sufficiently small $\varepsilon > 0$ its ε-neighborhood U_ε is isolating for both gradient flows $\operatorname{grad} H(\boldsymbol{x}, \pm 1)$.

By our assumption, the Morse indices and, therefore, the Conley indices are different for $\alpha = 1$ and $\alpha = -1$. Since the Conley index is invariant under continuous deformations of the flow (see property 3), such a situation is only possible when at some value of α the neighbourhood U_ε ceases to be isolating. This means the following. Either at the boundary of this neighborhood there is a singular point of the gradient flow (which proves the theorem) or there is a trajectory $\gamma(t)$ passing through some point of ∂U_ε which is entirely contained in this neighborhood. Let $\boldsymbol{x}_\pm$ be the limit points of the trajectory $\gamma(t)$ as $t \to \pm\infty$. Since we deal with a gradient flow, the points $\boldsymbol{x}_+$ and $\boldsymbol{x}_-$ are different and singular for the function H. Thus, inside the neighborhood there are at least two distinct singular points, which the theorem actually states. □

From the viewpoint of dynamics the critical points of a Hamiltonian, which are singular points of the Hamiltonian vector field, can be divided into types not only depending on the index but also depending on the nature of the eigenvalues of the linearized system. In the case of two degrees of freedom there are four such types:

1. center–center (two pairs of purely imaginary eigenvalues $\pm iA$, $\pm iB$),
2. center–saddle (a pair of purely imaginary and a pair of real eigenvalues $\pm iA$, $\pm B$),
3. saddle–saddle (two pairs of real eigenvalues $\pm A$, $\pm B$),
4. focus–focus (a quadruple of complex eigenvalues $\pm A \pm iB$).

The relation between these types and the Morse index is as follows:

– the point of center–center type can have any even index, i.e. 0, 2 or 4;
– the point of center–saddle type can have index 1 or 3;
– the points of saddle–saddle and focus–focus type always have index 2.

As we have seen above, under a deformation of the system the change of the Morse index is necessarily accompanied by the birth of new equilibrium points or by the disappearance of the old ones. Does an analogous event happen under the change of the type of the singular point? Taking into account the relation between the index and the type, this question can be put in a more precise form as follows:

> *can the point of index 2 change its type under deformation, for example, from center–center to focus–focus or saddle–saddle type, and if it can, does it imply the birth or elimination of singular points?*

To answer the first half of the question, it is convenient to depict regions corresponding to different types of singular points on the plane $\mathbb{R}^2 = \{(a, b)\}$, where a and b are the coefficients of the characteristic polynomial of the linearized Hamiltonian system:

$$\mathcal{X}(\lambda) = \lambda^4 + a\lambda^2 + b.$$

These regions are separated by the curve $a^2 - 4b = 0$ and the straight line $b = 0$ (see Fig. 14). Under a change of the parameter α the curve $\widetilde{\sigma}(\alpha) = (a(\alpha), b(\alpha))$ arises for the corresponding family of critical points $\boldsymbol{x}^{(0)}(\alpha)$ on this plane. It can be seen from Fig. 14 that in a typical situation the point with $\operatorname{ind}_M = 2$ can turn either from a focus–focus into a saddle–saddle or from a focus–focus into a center–center (and vice versa). Notice that in the generic case no additional singular points arise or disappear; however, periodic trajectories arise under the deformation of a focus–focus into a center-center. Sometimes this bifurcation is called the Hamiltonian Hopf bifurcation [27]. On the bifurcation diagram in the plane $\mathbb{R}^2 = \{(\alpha, H)\}$ (see the following section) we will not be able to notice bifurcations of this type.

Transformation of a center–center into a saddle–saddle is also possible, but this bifurcation is not generic.

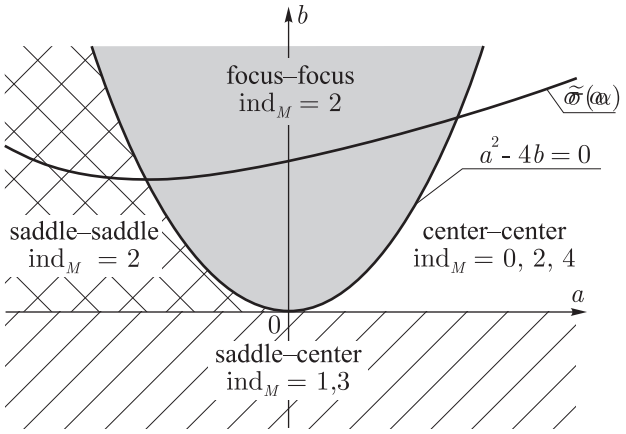

Fig. 14. Regions on the plane of coefficients of the characteristic polynomial which correspond to different types of fixed points, and a typical curve $\widetilde{\sigma}(\alpha)$ corresponding to a family of fixed points $\mathrm{ind}_M = 2$.

3.2. Bifurcation Diagram and Its Analysis

Many problems in mechanics often require finding and analyzing the equilibria of Hamiltonian systems depending on some parameter. In fact, this reduces to analysis of critical points of the Hamiltonian $H(\boldsymbol{x}, \alpha)$, which is a smooth (analytical) function of phase variables $\boldsymbol{x} \in \mathbb{R}^n$ and the parameter α.

One of the most common problems is to describe the relative equilibria of a Hamiltonian system possessing a cyclic integral (see the following section for more details). In this case one needs to find critical points of the Hamiltonian $H(\boldsymbol{x}, \alpha)$ reduced by the action of the integral, where α is the value of the cyclic integral. As a rule, for almost all values of α the critical points turn out to be nondegenerate and form one-parameter families $\boldsymbol{x}^{(i)}(\alpha)$, $i = 1, \ldots, m$. Note that on the plane of values of the first integrals $\mathbb{R}^2 = \{(\alpha, H)\}$ one can construct in a natural way the bifurcation curves σ_i corresponding to the singular points. These curves σ_i are given as graphs of the functions

$$h_i(\alpha) = H(\boldsymbol{x}^{(i)}(\alpha), \alpha).$$

After calculating the Morse indices of the Hamiltonian for the corresponding families of singular points $\boldsymbol{x}^{(i)}(\alpha)$, we can place them on the corresponding curves σ_i and track their change under variation of α. This diagram is called the *bifurcation diagram of the system*.

The problem often lies in the fact that we have only partial information on the critical points of H, i.e. we do not have their complete description. In order to avoid mistakes and "predict" a correct result, it is important to understand possible scenarios of change of the index when the point is moving along a branch of the bifurcation diagram. Thus, the theorem formulated above can help, for example, in the following situation. Assume that a one-parameter family of equilibrium points $\boldsymbol{x}^{(0)}(\alpha)$ (smooth in α) is given and we know that after passing through some value of the parameter α_0 the Morse index of $\boldsymbol{x}^{(0)}(\alpha)$ has changed. This means that at this moment the "birth" of some new family of singular points must happen. In other words, partial information about some equilibria can entail the existence of other equilibrium points.

For illustration, we consider again the second example with the function (3.1) and assume that only one family of singular points $\boldsymbol{x}^{(0)}(\alpha) = (0, 0)$ is known to us. We construct the corresponding bifurcation curve $\sigma_0\colon h_0(\alpha) = 0$, $\alpha \in [-1, 1]$ (Fig. 15a); we see that, according to Theorem 3, this diagram is not complete. A complete diagram should contain the curves corresponding to the equilibria $\boldsymbol{x}^{(1)}(\alpha)$ and $\boldsymbol{x}^{(2)}(\alpha)$ that were "born" at $\alpha = 0$. In this case, both families $\boldsymbol{x}^{(1)}(\alpha)$ and $\boldsymbol{x}^{(2)}(\alpha)$ are mapped to the same curve $\sigma_1\colon h_0(\alpha) = -\dfrac{\alpha^2}{2}$ (see Fig. 15b).

Remark. Actually, a more detailed study of the Conley index also provides insight into the "interaction" of indices of various families of singular points meeting at some bifurcation point, which makes it possible to formulate correct hypotheses and to test the results obtained in the study of a specific system.

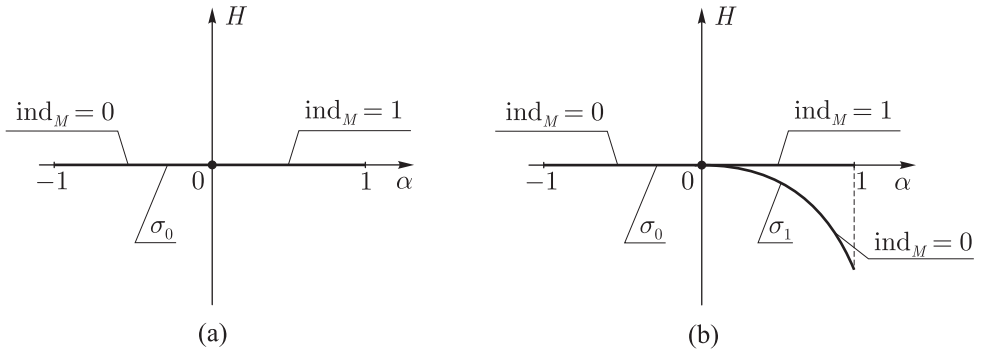

Fig. 15. Bifurcation diagram of system (3.1).

We point out another simple idea which is often used in the analysis of bifurcation diagrams. Suppose there are two families of critical points of the Hamiltonian $H(\boldsymbol{x},\alpha)$, which we denote by $\boldsymbol{x}^{(1)}(\alpha)$ and $\boldsymbol{x}^{(2)}(\alpha)$, so that the corresponding bifurcation curves on the plane (α, H) are determined by the graphs of the functions $h_1(\alpha) = H(\boldsymbol{x}^{(1)}(\alpha),\alpha)$, $h_2(\alpha) = H(\boldsymbol{x}^{(2)}(\alpha),\alpha)$.

If for some $\alpha = \alpha_0$ these families intersect in the phase space, i.e. $\boldsymbol{x}^{(1)}(\alpha_0) = \boldsymbol{x}^{(2)}(\alpha_0)$, then the bifurcation curves corresponding to them intersect for $\alpha = \alpha_0$ and are tangent to each other at the intersection point:

$$h_1(\alpha_0) = h_2(\alpha_0), \quad \frac{dh_1}{d\alpha}(\alpha_0) = \frac{dh_2}{d\alpha}(\alpha_0).$$

To prove it, it is sufficient to calculate the derivative along the bifurcation curves taking into account the condition that the points $\boldsymbol{x}^{(i)}(\alpha)$ are all critical:

$$\frac{dh_i}{d\alpha} = \frac{\partial H(\boldsymbol{x},\alpha)}{\partial\alpha}\bigg|_{\boldsymbol{x}=\boldsymbol{x}^{(i)}(\alpha)} + \left(\sum_k \frac{\partial H(\boldsymbol{x},\alpha)}{\partial x_k}\frac{dx_k^{(i)}(\alpha)}{d\alpha}\right)\bigg|_{\boldsymbol{x}=\boldsymbol{x}^{(i)}(\alpha)} = \frac{\partial H(\boldsymbol{x}^{(i)}(\alpha),\alpha)}{\partial\alpha},$$

hence, if $\boldsymbol{x}^{(1)}(\alpha_0) = \boldsymbol{x}^{(2)}(\alpha_0)$, then $\dfrac{dh_1}{d\alpha}(\alpha_0) = \dfrac{dh_2}{d\alpha}(\alpha_0)$ as well.

This is illustrated in Fig. 15b, where the intersection of three families of singular points $\boldsymbol{x}^{(0)}(\alpha)$, $\boldsymbol{x}^{(1)}(\alpha)$ and $\boldsymbol{x}^{(2)}(\alpha)$ corresponds to the merging of two branches σ_0 and σ_1 for $\alpha = 0$.

It follows from this assertion that if on the bifurcation diagram the branches intersect transversally, the corresponding families of critical points are separated from each other in the phase space.

As an example, we consider the function

$$H(q,p,\alpha) = p^2 + q^4 + \frac{4}{3}\alpha q^3 - q^2, \quad \alpha\in[-1,1], \tag{3.2}$$

possessing for all α three families of singular points

$$\boldsymbol{x}^{(0)}(\alpha) = (0,0), \quad \boldsymbol{x}^{(1)}(\alpha) = \left(0, -\frac{\alpha}{2} + \frac{\sqrt{\alpha^2+2}}{2}\right), \quad \boldsymbol{x}^{(2)}(\alpha) = \left(0, -\frac{\alpha}{2} - \frac{\sqrt{\alpha^2+2}}{2}\right).$$

The corresponding bifurcation diagram contains three different curves $\sigma_0 : h_0(\alpha) = 0$, $\sigma_1 : h_1(\alpha) = -\dfrac{\alpha^4}{6} - \dfrac{\alpha^2}{2} - \dfrac{1}{4} + \dfrac{\alpha(\alpha^2+2)^{3/2}}{6}$, $\sigma_2 : h_2(\alpha) = -\dfrac{\alpha^4}{6} - \dfrac{\alpha^2}{2} - \dfrac{1}{4} - \dfrac{\alpha(\alpha^2+2)^{3/2}}{6}$ (see Fig. 16). As is clear from the figure, the curves σ_1 and σ_2 intersect at $\alpha = 0$, although the corresponding families of critical points $\boldsymbol{x}^{(1)}(\alpha)$ and $\boldsymbol{x}^{(2)}(\alpha)$ do not have any common points in the phase space $\mathbb{R}^2 = \{(q,p)\}$.

The following section serves as an illustration of these ideas.

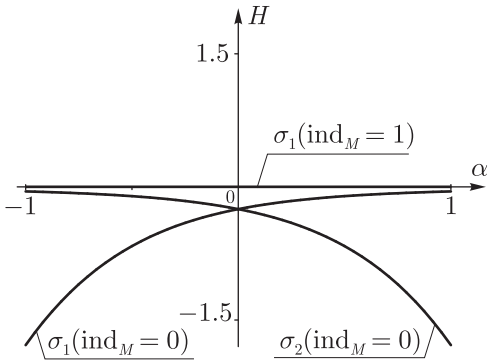

Fig. 16. Bifurcation diagram of system (3.2).

4. RELATIVE EQUILIBRIA IN THE PROBLEM OF THREE VORTICES IN A CIRCLE

4.1. Equations of Motion and Reduction

As an example, we consider a system describing the dynamics of three equal point vortices in a circular domain on a plane. Let us choose the origin of a fixed coordinate system O to coincide with the center of a circle, assume the vortex intensities to be equal to 1 and let their position be given by polar coordinates r_k, φ_k (see Fig. 17). Then the equations of motion are expressed in Hamiltonian form [4]

$$\begin{gathered}\dot r_k = \{r_k, H\} = \frac{1}{r_k}\frac{\partial H}{\partial \varphi_k}, \quad \dot\varphi_k = \{\varphi_k, H\} = -\frac{1}{r_k}\frac{\partial H}{\partial r_k}, \quad k = 1,2,3,\\ H = -\frac{1}{4\pi}\sum_{k<j}^{3} \ln \frac{r_k^2 + r_j^2 - 2r_k r_j \cos(\varphi_k - \varphi_j)}{R^4 + r_k^2 r_j^2 - 2R^2 r_k r_j \cos(\varphi_k - \varphi_j)} + \frac{1}{4\pi}\sum_{k=1}^{3} \ln(R^2 - r_k^2),\end{gathered} \tag{4.1}$$

where the Poisson bracket is defined by $\{r_k, \varphi_j\} = \frac{\delta_{kj}}{r_k}$.

The equations of motion for vortices (4.1) admit an additional first integral of motion — the *moment of vorticity*, which in this case can be written as

$$I = \frac{1}{2}\sum_{k=1}^{3} r_k^2. \tag{4.2}$$

The existence of this integral is a consequence of invariance of the equations of motion with respect to rotations around the center of the circle.

To find relative equilibria, we carry out a reduction by symmetry; to do so, we pass to the new variables ρ_k, ψ_k, $k = 1,2,3$, $I = \rho_3$ using the formulae

$$\begin{gathered}\psi_1 = \varphi_1 - \varphi_3, \quad \psi_2 = \varphi_2 - \varphi_3, \quad \psi_3 = \varphi_3,\\ \rho_1 = r_1^2/2, \quad \rho_2 = r_2^2/2, \quad \rho_3 = I = (r_1^2 + r_2^2 + r_3^2)/2,\end{gathered} \tag{4.3}$$

where $\psi_k \in (-\pi, \pi)$, $k = 1,2,3$, are the angle variables (see Fig. 17).

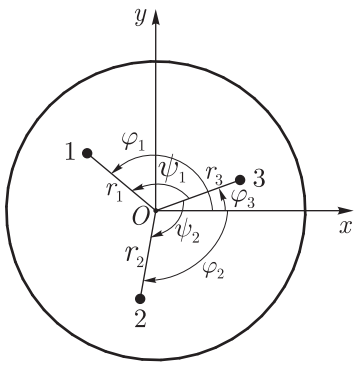

Fig. 17. Definition of variables.

It can be shown that the new coordinates are canonical:

$$\{\rho_1, \psi_1\} = \{\rho_2, \psi_2\} = \{I, \psi_3\} = 1,$$

the remaining brackets are equal to zero.

Throughout the rest of the paper, we shall assume without loss of generality that

$$R = 1.$$

Note that the regions of change of variables (4.3) and of the moment integral (4.2) are explicitly given as follows:

$$0 < \rho_k < 1/2, \quad -\pi < \psi_k < \pi,$$
$$k = 1, 2, \quad 0 < I < 3/2.$$

Expressing the coordinates of the vortices from (4.3)

$$\begin{gathered}\varphi_1 = \psi_1 + \psi_3, \quad \varphi_2 = \psi_2 + \psi_3, \quad \varphi_3 = \psi_3, \\ r_1 = \sqrt{2\rho_1}, \quad r_2 = \sqrt{2\rho_2}, \quad r_3 = \sqrt{2(I - \rho_1 - \rho_2)}\end{gathered} \tag{4.4}$$

and substituting them into the Hamiltonian (4.1), we obtain

$$\begin{aligned}H = &-\frac{3}{4\pi}\ln 2 + \frac{1}{4\pi}\big[\ln(1-2\rho_1) + \ln(1-2\rho_2) + \ln(1-2(I-\rho_1-\rho_2))\big] \\ &-\frac{1}{4\pi}\Bigg[\ln\frac{\rho_1+\rho_2-2\sqrt{\rho_1\rho_2}\cos(\psi_1-\psi_2)}{1+4\rho_1\rho_2-4\sqrt{\rho_1\rho_2}\cos(\psi_1-\psi_2)} \\ &+\ln\frac{I-\rho_1-2\sqrt{\rho_2(I-\rho_1-\rho_2)}\cos\psi_2}{1+4\rho_2(I-\rho_1-\rho_2)-4\sqrt{\rho_2(I-\rho_1-\rho_2)}\cos\psi_2} \\ &+\ln\frac{I-\rho_2-2\sqrt{\rho_1(I-\rho_1-\rho_2)}\cos\psi_1}{1+4\rho_1(I-\rho_1-\rho_2)-4\sqrt{\rho_1(I-\rho_1-\rho_2)}\cos\psi_1}\Bigg].\end{aligned} \tag{4.5}$$

Thus, the Hamiltonian function is independent of ψ_3, i.e. the variable ψ_3 is cyclic. Hence, the equations of motion governing the evolution of the variables ρ_1, ρ_2, ψ_1 and ψ_2 are separated and written in the canonical Hamiltonian form

$$\dot\rho_k = \frac{\partial H(I,\rho_1,\rho_2,\psi_1,\psi_2)}{\partial\psi_k}, \quad \dot\psi_k = -\frac{\partial H(I,\rho_1,\rho_2,\psi_1,\psi_2)}{\partial\rho_k}, \quad k = 1, 2. \tag{4.6}$$

Thus, we have carried out a reduction of the initial system to the two-degree-of-freedom Hamiltonian system (4.6) parametrically depending on the value of the first integral I.

As is well known, the relative equilibria, *i.e. the periodic solutions of the system* (4.1), are fixed points of the reduced system (4.6) and, consequently, are determined by the critical points of the Hamiltonian (4.5).

4.2. The Well-known Stationary Configurations and the Bifurcation Diagram

a. The well-known configurations. Two stationary configurations of three vortices in a circular domain are well known:

- *equilateral triangle* (*Thomson's configuration*) (Fig. 18a);
- *symmetric collinear configuration* (Fig. 18b).

Remark. Such configurations also exist in the general problem of N equal vortices (an equilateral polygon and a collinear configuration symmetric about the center). Results on their stability are contained in [8, 9, 26]. In [9] it is stated that in the case of three vortices there is an isolated value of the parameter for which Thomson's configuration loses stability.

A natural question arises:
do these configurations exhaust all possible relative equilibria in this system?

Following the approach described in Section 3, primarily on the plane of values of the first integrals I and H, it is necessary to construct a bifurcation diagram of the system on which the families of critical points correspond to bifurcation curves.

Furthermore, we place the Morse index of the reduced Hamiltonian H (see Fig. 19) on the bifurcation curves. After such a modification the bifurcation diagram allows us to answer the questions concerning the existence, type and number of relative equilibria of the system under consideration.

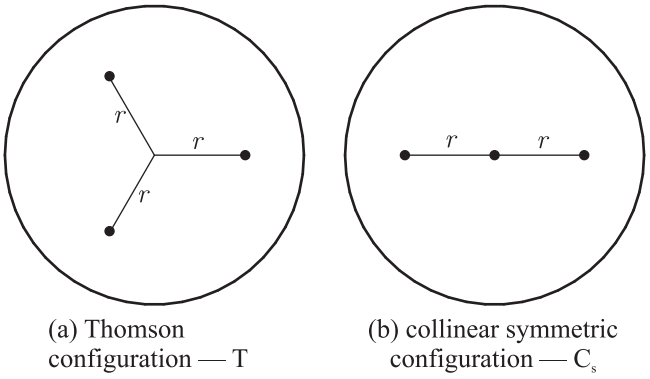

Fig. 18. The well-known stationary configurations of three vortices in a circle.

Remark. In some works the bifurcation diagram is also called the Smale diagram [13] or energy-momentum diagram [17] depending on the field of research. Some authors (see, e.g., [17]) call the method of stability analysis using a bifurcation diagram the energy–momentum method.

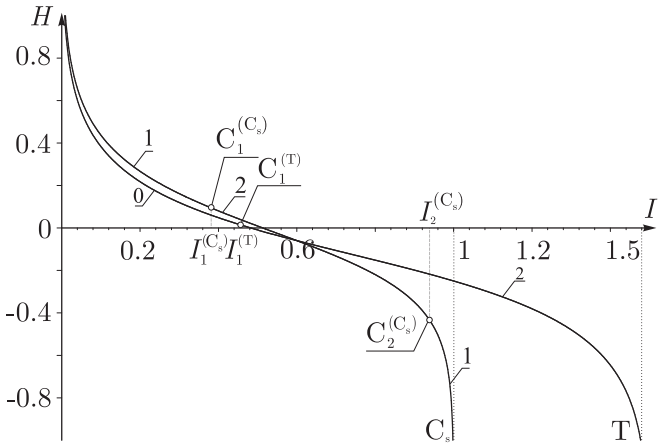

Fig. 19. Bifurcation curves for the well-known stationary configurations of three vortices in a circle (T — Thomson's configuration, C_s — collinear configuration).

The bifurcation curves of the well-known stationary configurations are constructed as follows.

Thomson's (*equilateral*) *configuration*, which we shall denote by the letter T, corresponds to two families of critical points of the Hamiltonian (4.5) defined by

$$\begin{aligned} &\textit{1st family}\colon\ \rho_1=\rho_2=\frac{I}{3},\quad \psi_1=\frac{2\pi}{3},\quad \psi_2=-\frac{2\pi}{3},\\ &\textit{2nd family}\colon\ \rho_1=\rho_2=\frac{I}{3},\quad \psi_1=-\frac{2\pi}{3},\quad \psi_2=\frac{2\pi}{3}, \end{aligned} \tag{4.7}$$

where the value of the moment integral I is a parameter of the family, it is related to the distance from the vortices to the center of the circle by the relation $r=\sqrt{\dfrac{2}{3}I}$. These two families correspond to reflection symmetric configurations.

The collinear symmetric configuration, which we denote by C_s, defines three families of critical points differing in the number of the vortex in the center of the circle

$$\begin{aligned} &\textit{1st family}: \ \rho_1 = \frac{I}{2}, \quad \rho_2 = 0, \quad \psi_1 = \pi, \\ &\textit{2nd family}: \ \rho_1 = 0, \quad \rho_2 = \frac{I}{2}, \quad \psi_2 = \pi, \\ &\textit{3rd family}: \ \rho_1 = \rho_2 = \frac{I}{2}, \end{aligned} \tag{4.8}$$

where I is a parameter of the family and is related to the distance from the non-central vortices to the center of the circle by the relation $r = \sqrt{I}$.

The variables (4.3) are unsuitable for analysis of the collinear symmetric configuration, since one of the vortices lies in the center of the circle, so that either one of the angles ψ_k or both cannot be determined immediately (this is analogous to the singularity at the origin of coordinates when polar coordinates are determined). Nevertheless, the canonical change of variables allows this problem to be solved; for example, for the first family in (4.8) it has the form

$$\sqrt{2\rho_2}\cos\psi_2 = X, \quad \sqrt{2\rho_2}\sin\psi_2 = Y, \quad \{X, Y\} = 1. \tag{4.9}$$

Since the initial system (for $\Gamma_1 = \Gamma_2 = \Gamma_3$) is symmetric with respect to permutations of the vortices, the results for the other two families turn out to be identical.

Due to the symmetry with respect to permutation of the vortices (which holds only for the case of equal intensities $\Gamma_1 = \Gamma_2 = \Gamma_3$) all five families of critical points for Thomson's and collinear symmetric configurations determine only two bifurcation curves on the plane of the integrals I and H, which can be represented as

$$\begin{aligned} &\textit{Thomson's configuration}: \ H(I) = \frac{3}{4\pi}\ln\frac{1-\left(\frac{2I}{3}\right)^3}{2I}, \\ &\textit{collinear configuration}: \ H(I) = \frac{1}{4\pi}\ln\frac{(1-I^2)^2}{4I^3}. \end{aligned} \tag{4.10}$$

Figure 19a shows a bifurcation diagram for Thomson's (T) and collinear (C_s) configurations. The regions of change of the moment integral (4.2) are determined by the inequalities

$$\begin{aligned} &0 \leqslant I \leqslant \frac{3}{2} \ \text{ for Thomson's configuration}, \\ &0 \leqslant I \leqslant 1 \ \text{ for the collinear configuration}. \end{aligned}$$

The left boundary ($I = 0$) corresponds to cases where all vortices lie in the center of the circle, the right boundary ($I = \frac{3}{2}$ and $I = 1$) corresponds to cases where the vortices touch the boundaries of the circle (except the central vortex for the collinear configuration). In all cases, the energy of configurations tends to $+\infty$ at the left boundary and to $-\infty$ at the right boundaries, therefore, as the integral I approaches these values, the bifurcation curves $H(I)$ corresponding to fixed points (see the bifurcation diagram in Fig. 19) exhibit asymptotic behavior.

Remark. For small values of the parameter I the bifurcation diagram for Thomson's and collinear configurations is isomorphic to the planar case.

As was shown above, each point on the bifurcation curves corresponds to several fixed points of system (4.6). This is also valid for other possible values (I_0, H_0) which do not lie on the curves, — as a rule, they correspond to several different components of the disconnected integral manifold $\mathcal{M}_{I_0,H_0} = \{\boldsymbol{z} \mid H(\boldsymbol{z}) = H_0,\ I(\boldsymbol{z}) = I_0\}$, where $\boldsymbol{z}$ denotes a set of phase variables of the system.

b. The indices of Thomson's and collinear symmetric configurations. Let us place the Morse index on a branch of the bifurcation diagram that corresponds to Thomson's configuration. To do so, we denote the variables of the reduced system by $\boldsymbol{x} = (\rho_1, \rho_2, t_1, t_2)$ and calculate the matrix of the quadratic part of the Hamiltonian $\mathbf{B} = \left\| \dfrac{\partial^2 H}{\partial x_i \partial x_j} \right\|$ for any of the families (4.8). At the points of change of the index the eigenvalues of the matrix $\mathbf{B}$ change sign (vanish), they are found from the equation $\det \mathbf{B} = 0$, which in this case has the form [9]

$$5p^6 + 9p^5 + 5p^3 + 9p^2 - 1 = 0, \quad p = r^2 = \frac{2}{3}I. \tag{4.11}$$

Only one root of this equation $I_1^{\mathrm{T}} \approx 0.456$ lies in the range of the moment integral $0 \leqslant I \leqslant \dfrac{3}{2}$. We denote the corresponding point on the bifurcation curve by $\mathrm{C}_1^{(\mathrm{T})}$. The calculation of the index on the left of the bifurcation point gives ind = 0 and on the right ind = 2 (Fig. 19).

Similarly, we find that the bifurcation points for the collinear symmetric configuration are determined by

$$(81p^7 + 27p^6 + 369p^5 + 54p^4 - 312p^3 + 144p - 32)(9p^4 + 27p^3 + 9p^2 - 12p - 4) = 0, \quad p = r^2 = \frac{2}{3}I. \tag{4.12}$$

In the range of the moment integral $0 \leqslant I \leqslant 1$ there are two bifurcation points $I_1^{\mathrm{C_s}} \approx 0.379$ and $I_2^{\mathrm{C_s}} \approx 0.938$ (we denote the corresponding curves on the bifurcation curve by $\mathrm{C}_1^{(\mathrm{C}_s)}$ and $\mathrm{C}_2^{(\mathrm{C}_s)}$). The calculation of the index of the quadratic part H gives the following results:

$$\begin{aligned}
&\mathrm{ind}_M = 1,\ I < I_1^{\mathrm{C_s}},\\
&\mathrm{ind}_M = 2,\ I_1^{\mathrm{C_s}} < I < I_2^{\mathrm{C_s}},\\
&\mathrm{ind}_M = 1,\ I > I_2^{\mathrm{C_s}}.
\end{aligned}$$

4.3. New Stationary Configurations and Their Stability

From Fig. 19, where the bifurcation curves T and $\mathrm{C_s}$ for Thomson's and collinear configurations are shown, it can be seen that

1) the curves T and $\mathrm{C_s}$ intersect transversally,
2) on the bifurcation curves T and $\mathrm{C_s}$ there are isolated points at which there occurs a change of the index of the critical points of the Hamiltonian which correspond to these curves.

Using the results of the previous section, we can draw the following conclusions:

1) *in the phase space, the critical points corresponding to different families* T and $\mathrm{C_s}$, *are isolated from each other for all values of the parameter* I (*since for nonisolated families the bifurcation curves at the point of merging or intersection are tangent to each other*);

2) *by Theorem* 3 *of an isolated family, at the points of change of the index there must arise new critical points corresponding to hitherto unknown configurations.*

We show that in this case the second scenario takes place, i.e. *new stationary configurations are born under the change of the index*.

It is clear that as the parameters change, the sought-for new configurations should tend to Thomson's or collinear symmetric configurations in such a way that the corresponding bifurcation curves on the plane I, H merge with the curves T and $\mathrm{C_s}$ at the points of change of the index. In addition, it is natural to expect that for new configurations the symmetry will decrease but not disappear completely (see, e.g., [15, 16]).

Possible configurations which satisfy these requirements are *isosceles* and *collinear asymmetric* configurations (Figs. 20a and 20b).

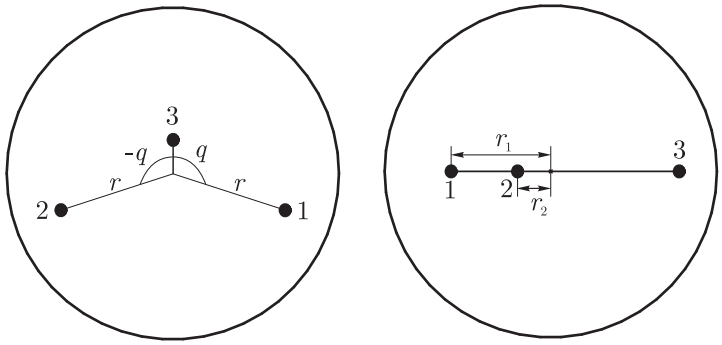

(a) isosceles configuration — T_{is} (b) collinear assymmetric configuration — C_n

Fig. 20. New stationary configurations of three vortices in a circle.

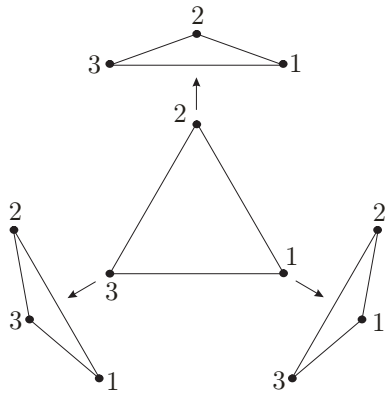

Fig. 21. Appearance of of isosceles configurations from Thomson's configurations.

c. Isosceles configuration In a neighborhood of each of two Thomson's configurations (which differ in the parity of permutation of the numbers of vortices) there may appear three isosceles configurations differing in the number of the vortex at the vertex (see Fig. 21).

Owing to the symmetry of the initial system with respect to permutations of the vortices it is sufficient to consider one of these six configurations. Thus, we shall seek the required family of critical points of the reduced Hamiltonian (4.5) in the form

$$\rho_1 = \rho_2 = \frac{r^2}{2}, \quad \psi_1 = -\psi_2 = q. \tag{4.13}$$

We denote the submanifold defined by these relations as

$$\mathcal{M}_{\text{is}} = \{(\rho_1, \rho_2, \psi_1, \psi_2) \mid \rho_2 = \frac{r^2}{2}, \psi_1 = -\psi_2 = q\}. \tag{4.14}$$

Substituting (4.14) into the conditions for extremality of the Hamiltonian (4.5), we obtain the following equations:

$$\begin{aligned} \left.\frac{\partial H}{\partial \rho_1}\right|_{\mathcal{M}_{\text{is}}} &= \left.\frac{\partial H}{\partial \rho_2}\right|_{\mathcal{M}_{\text{is}}} = R_{\text{is}}(r,q,I) = 0, \\ \left.\frac{\partial H}{\partial \psi_1}\right|_{\mathcal{M}_{\text{is}}} &= \left.\frac{\partial H}{\partial \psi_2}\right|_{\mathcal{M}_{\text{is}}} = \Psi_{\text{is}}(r,q,I) = 0. \end{aligned} \tag{4.15}$$

The functions $R_{\text{is}}(r,q,I)$, $\Psi_{\text{is}}(r,q,I)$ are rather unwieldy. Because of this, we do not present them here (they can easily be obtained from the Hamiltonian (4.5) using a package for analytical

computations, for example, Maple or Mathematica etc.). Solving this system for the variables r and q, we obtain a one-parameter family (or several families) of critical points parameterized by the value of the integral I, which corresponds to isosceles configurations.

It is impossible to obtain an exact analytical solution of system (4.15). Therefore, we shall solve it numerically by the method of continuation in terms of the parameter. Using the isosceles configuration as an example we describe this process in more detail.

First, we restrict the Hamiltonian (4.5) to the submanifold M_{is}:

$$H_{\text{is}} = -\frac{3}{4\pi}\ln 2 + \frac{1}{4\pi}\bigl[2\ln(1-r^2) + \ln(1-2(I-r^2))\bigr] \\ -\frac{1}{4\pi}\left[\ln\frac{r^2(1-\cos 2q)}{1+r^4-2r^2\cos 2q} + 2\ln\frac{2I-r^2-2r\sqrt{2(I-r^2)}\cos q}{2(1+2r^2(I-r^2)-2r\sqrt{2(I-r^2)}\cos q)}\right]. \tag{4.16}$$

By (4.15), the critical points of the initial Hamiltonian on the manifold M_{is} coincide with the critical points of H_{is}.

We then choose a value of the moment integral I_0 that is close to the bifurcation value I_1^{T}, and in a neighborhood of Thomson's configuration $z_{\text{T}}(I_0) = (r^2 = \frac{2}{3}I_0, q = \frac{2\pi}{3})$ we numerically find a critical point $z_*(I_0)$ of the Hamiltonian H_{is} which is different from $z_{\text{T}}(I_0)$. Next, we change the value of the moment integral by the small quantity $I_1 = I_0 + \delta$, and in a neighborhood of the found point $z_*(I_0)$ we find a new critical point $z_*(I_1)$. Continuing this procedure, we construct a family of critical points corresponding to the isosceles configuration $z_{\text{is}}(I)$. For the found families we construct bifurcation curves on the plane of the first integrals and specify the index of the complete Hamiltonian (4.5) for each of the branches.

Using the method described above, we have found two families (without considering the rearrangement of vortices) of isosceles configurations, which we denote by $\text{T}_{\text{is}}^{(1)}$ and $\text{T}_{\text{is}}^{(2)}$ (Figs. 22 and 23).

Remark. In view of the permutations of the vortices, it is necessary to multiply the number of the families of isosceles configurations by 6.

The found isosceles configurations possess the following properties (see Figs. 22 and 23):

– the family $\text{T}_{\text{is}}^{(1)}$ continues on both sides of the bifurcation point $\text{C}_1^{(\text{T})}$. For $I > I_1^{(\text{T})}$ it continues up to the point $\text{C}_2^{(\text{C}_\text{s})}$, where it merges with the family of collinear symmetric configurations, and for $I < I_1^{(\text{T})}$ it continues to the return point $I = I^{(\text{T}_{\text{is}})} \approx 0.442$, in which the second family of isosceles configurations $\text{T}_{\text{is}}^{(2)}$ is born,

– the family $\text{T}_{\text{is}}^{(2)}$ continues for $I > I^{(\text{T}_{\text{is}})}$ to the second return point as $I \to \frac{1}{2}$, at which it merges with the family of collinear asymmetric configurations (which will be described below),

– the index of the quadratic part of the Hamiltonian for the family $\text{T}_{\text{is}}^{(1)}$ is everywhere equal to 1 for $I \neq I_2^{(\text{T})}$,

– the index of the quadratic part of the Hamiltonian for $\text{T}_{\text{is}}^{(2)}$ is everywhere equal to 0.

Thus, using the numerical analysis of critical points of system (4.6), i.e. of relative equilibria of the initial system (4.1), we have proved the following theorem.

Theorem 4. *In the problem of three equal vortices in a circle there exist two* (*up to permutation of the vortices*) *families of isosceles stationary configurations* $\text{T}_{\text{is}}^{(1)}$ *and* $\text{T}_{\text{is}}^{(2)}$.

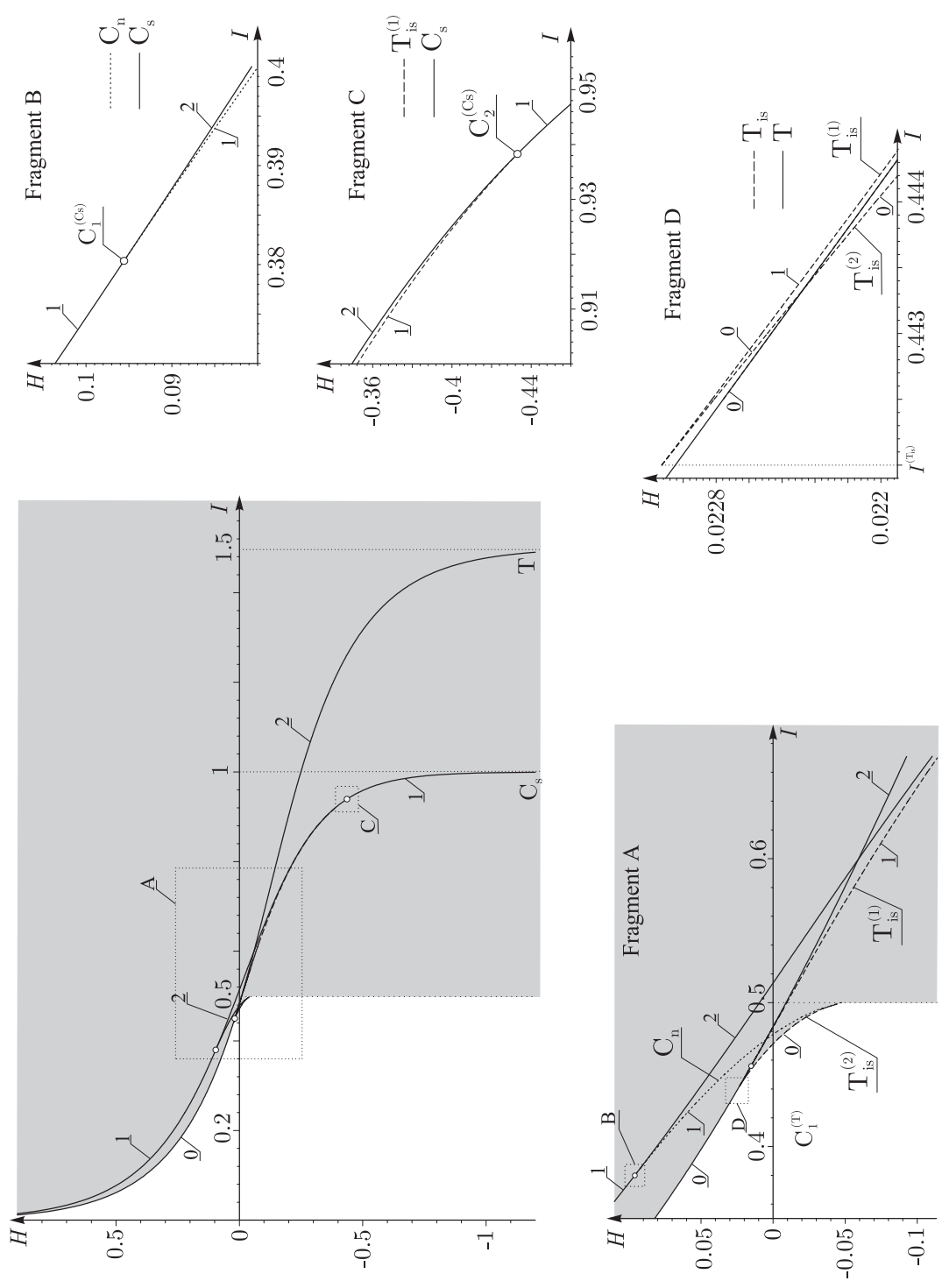

Fig. 22. Bifurcation diagram for stationary configurations of three vortices in a circle (T — Thomson's configuration, C_s — collinear symmetric configuration, T_{is} — isosceles configuration, C_n — collinear asymmetric configuration). Grey denotes a region of possible values of the integrals I, H.

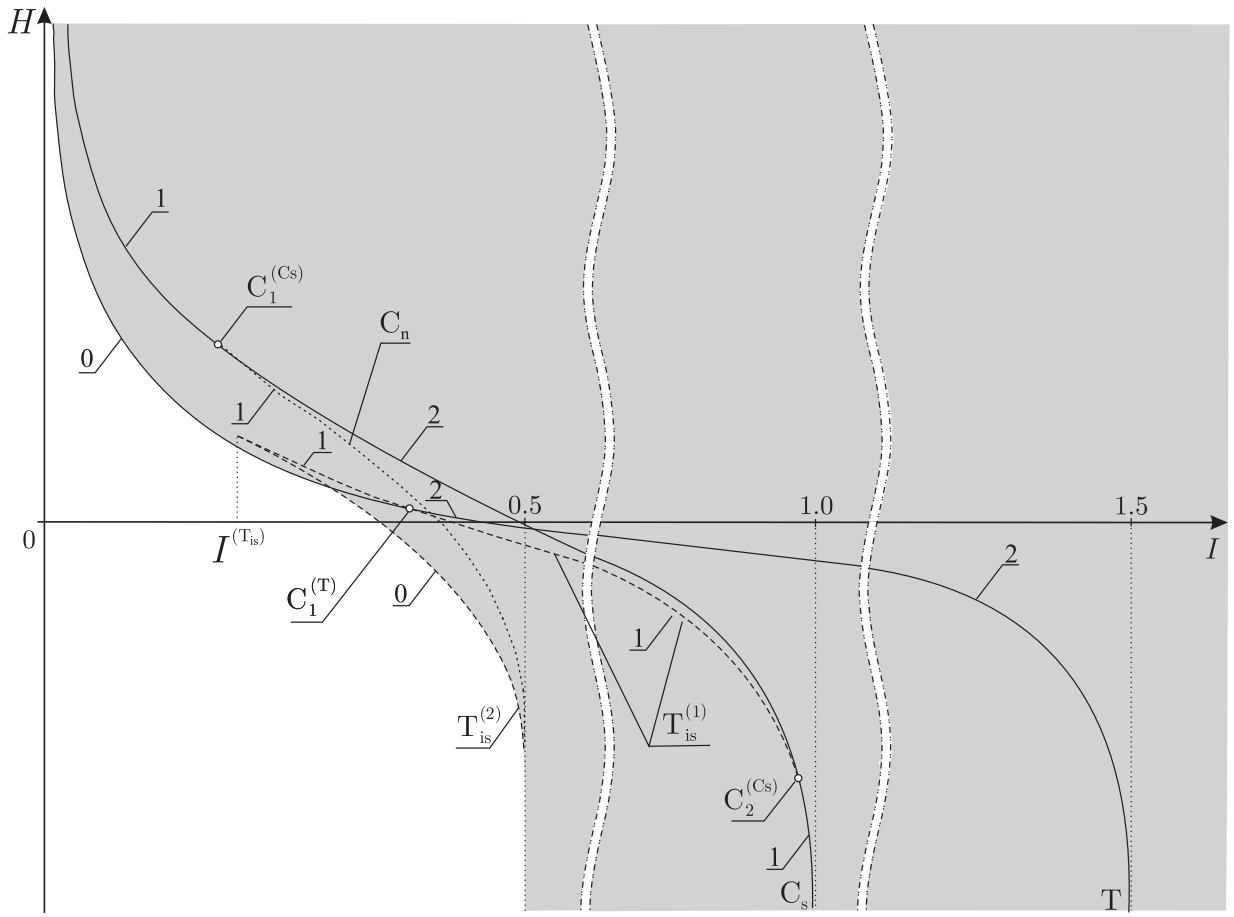

Fig. 23. A schematic bifurcation diagram (not to scale). Grey denotes a region of possible values of the integrals I, H.

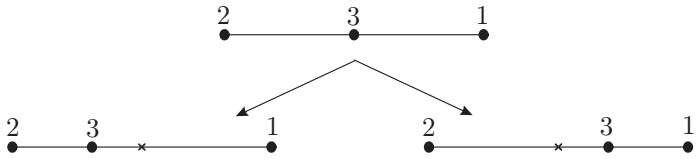

Fig. 24. Appearance of collinear asymmetric configurations.

d. Collinear asymmetric configuration. In a neighborhood of each of three collinear symmetric configurations which differ in the number of the vortex in the center there appear two collinear asymmetric configurations differing in the parity of permutation of the vortices and in the number of the vortex that lies on the other side of the other two vortices relative to the center (see Fig. 24).

Owing to the symmetry of the initial system with respect to permutations of the vortices, it is sufficient to consider one of these six configurations. Thus, we shall seek the required family of critical points of the reduced Hamiltonian (4.5) in the form

$$\rho_1 = \frac{r_1^2}{2}, \quad \rho_2 = \frac{r_2^2}{2}, \quad \psi_1 = \psi_2 = \pi. \tag{4.17}$$

We denote the submanifold defined by these relations as

$$\mathcal{M}_{\mathrm{n}} = \{(\rho_1, \rho_2, \psi_1, \psi_2) \mid \rho_1 = \frac{r_1^2}{2}, \rho_2 = \frac{r_2^2}{2}, \psi_1 = \psi_2 = \pi\}. \tag{4.18}$$

Substituting (4.18) into the conditions for extremality of the Hamiltonian (4.5), we obtain the following equations:

$$\left.\frac{\partial H}{\partial \rho_1}\right|_{\mathcal{M}_\mathrm{n}} = \left.\frac{\partial H}{\partial \rho_2}\right|_{\mathcal{M}_\mathrm{n}} = R_\mathrm{n}(r_1, r_2, I) = 0,$$
$$\left.\frac{\partial H}{\partial \psi_1}\right|_{\mathcal{M}_\mathrm{n}} = \left.\frac{\partial H}{\partial \psi_2}\right|_{\mathcal{M}_\mathrm{n}} = \Psi_\mathrm{n}(r_1, r_2, I) = 0. \tag{4.19}$$

We do not present here the functions $R_\mathrm{n}(r_1, r_2, I)$, $\Psi_\mathrm{n}(r_1, r_2, I)$ either, since they are unwieldy. Solving this system by the method of continuation in terms of the parameter for the variables r_1 and r_2, we obtain one family of critical points (we shall denote it by $\mathrm{C_n}$), which is parametrized by the value of the integral I and corresponds to the collinear asymmetric configurations. For the found family we construct a bifurcation curve on the plane of the first integrals and specify the index of the quadratic part of the Hamiltonian (4.5) (Fig. 22).

Remark. In view of the permutations it is necessary to multiply the number of the families of collinear asymmetric configurations by 6 too.

The found collinear asymmetric configurations possess the following properties (see Fig. 23):

- the family $\mathrm{C_n}$ is born at the point $I = I_1^{(\mathrm{C_s})}$ and continues to the return point as $I \to \frac{1}{2}$, at which it merges with the family of isosceles configurations $\mathrm{T}_\mathrm{is}^{(2)}$,
- the index of the quadratic part of the Hamiltonian for $\mathrm{C_n}$ is everywhere equal to 1.

Thus, using the numerical analysis of critical points of system (4.6), we have proved the following theorem.

Theorem 5. *In the problem of three equal vortices in a circle there exists one* (*up to permutation of the vortices*) *family* $\mathrm{C_n}$ *of collinear asymmetric stationary configurations.*

5. DISCUSSION

It is interesting to compare the results obtained for three vortices of equal intensity in a circle with analogous results of A. Albouy in the problem of four equal vortices on a plane [15, 16]. In particular, A. Albouy showed that there is a stationary configuration in which three vortices form an isosceles triangle and the fourth one lies on its axis of symmetry; in the case of vortices in a circle, the center of the circle plays the role of the fourth vortex.

We point out another result that one can also try to generalize to the problem we consider. This is the theorem on the finiteness of the number of relative equilibria in the problem of four vortices on a plane with arbitrary intensities [25]. For vortices in a circle the question of finiteness of the number of stationary configurations with arbitrary intensities requires additional research, since the homogeneity of the equations of motion is used essentially in the proofs of [25].

In conclusion, we point out that it would be interesting to apply the methods developed in this paper to the search for and analysis of partial solutions in nonconservative models of vortex dynamics (in particular, to the problems of the dynamics of point vortex sources [19] and dissipating vortices [32]).

The authors are grateful to A. A. Kilin and S. M. Gusein-Zade for useful discussions in the course of work.

This research was supported by the Grant of the Government of the Russian Federation for state support of scientific research conducted under supervision of leading scientists in Russian educational institutions of higher professional education (contract no. 11.G34.31.0039) and the federal target programme “Scientific and Scientific-Pedagogical Personnel of Innovative Russia” (14.740.11.0876). The work was supported by the Grant of the President of the Russian Federation for the Leading Scientific Schools of the Russian Federation (NSh-2519.2012.1).

REFERENCES

1. Anosov, D. V., Aranson, S. Kh., Bronstein, I. U., and Grines, V. Z., Smooth Dynamical Systems, in *Ordinary Differential Equations and Smooth Dynamical Systems,* D. V. Anosov, V. I. Arnol'd (Eds.), Encyclopaedia Math. Sci., vol. 1, Berlin: Springer, 1988.
2. Bolsinov, A. V., Borisov, A. V., and Mamaev, I. S., Hamiltonisation of Non-Holonomic Systems in the Neighborhood of Invariant Manifolds, *Regul. Chaotic Dyn.*, 2011, vol. 16, no. 5, pp. 443–464. [Original Russian version: *Rus. J. Nonlin. Dyn.,* 2010, vol. 6, no. 4, pp. 829–854].
3. Bolsinov, A. V., Borisov, A. V., and Mamaev, I. S., Topology and Stability of Integrable Systems, *Uspekhi Mat. Nauk,* 2010, vol. 65, no. 2, pp. 71–132 [*Russian Math. Surveys,* 2010, vol. 65, no. 2, pp. 259–318].
4. Borisov, A. V. and Mamaev, I. S., *Mathematical Methods in the Dynamics of Vortex Structures,* Moscow–Izhevsk: R&C Dynamics, Institute of Computer Science, 2005 (Russian).
5. Dubrovin, B. A., Fomenko, A. T., and Novikov, S. P., *Modern Geometry: Methods and Applications: Part 1. The Geometry of Surfaces, Transformation Groups, and Fields,* 2nd ed., Grad. Texts in Math., vol. 93, New York: Springer, 1992;
   Dubrovin, B. A., Fomenko, A. T., and Novikov, S. P., *Modern Geometry: Methods and Applications: Part 2. The Geometry and Topology of Manifolds,* Grad. Texts in Math., vol. 104, New York: Springer, 1985.
6. Katok, S. B., Bifurcation Sets and Integral Manifolds in the Problem of Motion of a Heavy Rigid Body, *Uspekhi Mat. Nauk,* 1972, vol. 27, no. 2, pp. 126–132 (Russian).
7. Borisov, A. V., Mamaev, I. S., and Kilin, A. A., Dynamics of Point Vortices in and around a Circular Domain, in *Fundamental and Applied Problems in the Theory of Vortices,* A. V. Borisov, I. S. Mamaev, M. A. Sokolovskiy (Eds.), Moscow–Izhevsk: R&C Dynamics, Institute of Computer Science, 2003, pp. 414–440 (Russian).
8. Kurakin, L. G., Stability, Resonances, and Instability of the Regular Vortex Polygons in the Circular Domain, *Dokl. Akad. Nauk,* 2004, vol. 399, no. 1, pp. 52–55 [*Dokl. Phys.,* 2004, vol. 49, no. 11, pp. 658–661].
9. Kurakin, L. G., The Stability of Thomson's Configurations of Vortices in a Circular Domain, *Rus. J. Nonlin. Dyn.,* 2009, vol. 5, no. 3, pp. 295–317 (Russian).
10. Markeev, A. P., *Theoretical Mechanics,* Moscow–Izhevsk: R&C Dynamics, Institute of Computer Science, 2007 (Russian).
11. Moser, J., *Lectures on Hamiltonian Systems,* Mem. Amer. Math. Soc., vol. 81, Providence, RI: AMS, 1968.
12. Smale, S., Topology and Mechanics: 1, *Invent. Math.,* 1970, vol. 10, no. 4, pp. 305–331;
    Smale, S., Topology and Mechanics: 2. The Planar n-Body Problem, *Invent. Math.,* 1970, vol. 11, no. 1, pp. 45–64.
13. Tatarinov, Ya. V., Portraits of the Classical Integrals of the Problem of Rotation of a Rigid Body about a Fixed Point, *Vestn. Moskov. Univ., Ser. 1. Mat. Mekh.,* 1974, vol. 6, pp. 99–105 (Russian).
14. Fomenko, A. T. and Fuks, D. B., *A Course in Homotopic Topology,* Moscow: Nauka, 1989 (Russian).
15. Albouy, A., Symétrie des configurations centrales de quatre corps, *C. R. Acad. Sci. Paris, Sér. 1,* 1995, vol. 320, pp. 217–220.
16. Albouy, A., The Symmetric Central Configurations of Four Equal Masses, *Contemp. Math.,* 1996, vol. 198, pp. 131–135.
17. Arango, C. A. and Ezra, G. S., Classical Mechanics of Dipolar Asymmetric Top Molecules in Collinear Static Electric and Nonresonant Linearly Polarized Laser Fields: Energy-Momentum Diagrams, Bifurcations and Accessible Configuration Space, arXiv:physics/0611231v1 [physics.class-ph], 23 Nov 2006.
18. Armstrong, M. A., *Basic Topology,* New York: Springer, 1983.
19. Borisov, A. V. and Mamaev, I. S., On the Problem of Motion of Vortex Sources on a Plane, *Regul. Chaotic Dyn.,* 2006, vol. 11, no. 4, pp. 455–466.
20. Charles Conley Memorial Volume: Special Issue of Ergodic Theory and Dynamical Systems, *Ergodic Theory Dynam. Systems,* 1988, vol. 8/8*, no. 9.
21. Conley, Ch., *Isolated Invariant Sets and the Morse Index,* CBMS Regional Conference Series in Mathematics, vol. 38, Providence, R. I.: AMS, 1978.
22. Conley, Ch. C. and Zehnder, R., Morse-Type Index Theory for Flows and Periodic Solutions for Hamiltonian Equations, *Comm. Pure Appl. Math.,* 1984, vol. 37, no. 2, pp. 207–253.
23. Grauert, H., On Levi's Problem and the Imbedding of Real-Analytic Manifolds, *Ann. of Math. (2),* 1958, vol. 68, pp. 460–472.
24. Guckenheimer, J. and Holmes, Ph., *Nonlinear Oscillations, Dynamical Systems and Bifurcations of Vector Fields,* New York: Springer, 1983.
25. Hampton, M. and Moeckel, R., Finiteness of Stationary Configurations of the Four-Vortex Problem, *Trans. Amer. Math. Soc.,* 2009, vol. 361, pp. 1317–1332.
26. Havelock, T. H., The Stability of Motion of Rectilinear Vortices in Ring Formation, *Philos. Mag.,* 1931, vol. 11, no. 70, pp. 617–633.

27. van der Meer, J.-C., *The Hamiltonian Hopf Bifurcation,* Lecture Notes in Math., vol. 1160, Berlin: Springer, 1985.
28. Milnor, J. W., *Topology from the Differentiable Viewpoint: Based on Notes by David W. Weaver,* Princeton, NJ: Princeton Univ. Press, 1997.
29. Mischaikow, K., The Conley Index Theory: A Brief Introduction, in *Conley Index Theory (Warsaw, 1997),* Banach Center Publ., vol. 47, Warsaw: Polish Acad. Sci., 1999, pp. 9–19.
30. Mischaikow, K. and Mrozek, M., Conley Index Theory, in *Conley Index: Handbook of Dynamical Systems: Vol. 2: Towards Applications,* B. Fiedler (Ed.), Amsterdam: Elsevier, 2002, pp. 393–460.
31. O'Neil, K., Clustered Equilibria of Point Vortices, *Regul. Chaotic Dyn.,* 2011, vol. 16, no. 6, pp. 555–561.
32. Shashikanth, B. N., Dissipative N-Point-Vortex Models in the Plane, *J. Nonlinear Sci.,* 2010, vol. 20, no. 1, pp. 81–103.
33. Yatsuyanagi, Yu., Kiwamoto, Ya., Tomita, H., Sano, M. M., Yoshida, T., and Ebisuzaki, T., Dynamics of Two-Sign Point Vortices in Positive and Negative Temperature State, *Phys. Rev. Lett.,* 2005, vol. 94, 054502, 4 pp.